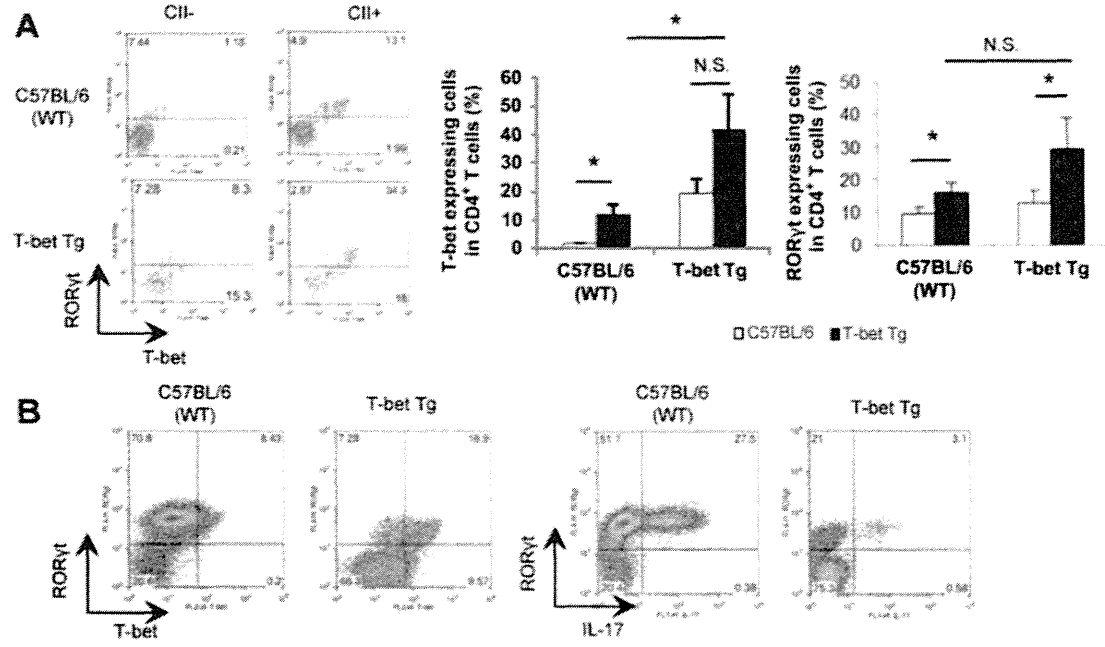

Figure 3. Suppression of Th17 cell differentiation by enforced expression of T-bet in T cells despite expression of retinoic acid receptor–related orphan nuclear receptor γt (RORγt). **A**, Ten days after the first type II collagen (CII) immunization, lymphocytes derived from the draining lymph nodes of C57BL/6 (wild-type [WT]) and T-bet–transgenic (Tg) mice were cultured for 72 hours in the presence or absence of 100 μg/ml of denatured CII. Levels of T-bet and RORγt expression on CD4+ T cells were analyzed by intracellular staining. Numbers in each compartment of the histograms are the percentage of transcription factor–expressing cells gated on CD4+ T cells. Values in the bar graphs are the mean ± SD of 3 mice per group. * = $P < 0.05$ by Student's *t*-test. NS = not significant. **B**, CD4+ T cells were isolated from the spleen of C57BL/6 and T-bet–Tg mice by magnetic-activated cell sorting and were then cultured for 96 hours with soluble anti-CD3 antibody, soluble anti-CD28 antibody, interleukin-6 (IL-6), and transforming growth factor β. Cytokine production and transcription factor expression on CD4+ T cells were analyzed by intracellular staining. Representative histograms from flow cytometric analysis of T-bet and RORγt expression with IL-17 production are shown. Numbers in each compartment are the percentage of positive cells gated on CD4+ T cells.

spleen of T-bet–Tg mice as compared with B6 mice (Figures 4A and B). The absolute number of CD4+ and CD8+ T cells also tended to be lower in T-bet–Tg mice (Figure 4B). Moreover, analysis of the thymus showed a significantly low number of total thymocytes in T-bet–Tg mice and the presence of an abnormal proportion of T precursor cells, such as a low number of double-positive T cells and CD4 single-positive T cells in T-bet–Tg mice (Figure 4C). These results suggest abnormal T cell development in the thymus of T-bet–Tg mice.

Inhibition of IL-17 production by CII-reactive CD4+ T cells in T-bet–Tg mice. To clarify whether T-bet overexpression on CD4+ T cells directly affects cytokine production, we performed criss-cross experiments using CD4+ T cells from B6 and T-bet–Tg mice, as well as DCs from B6 and T-bet–Tg mice in CII–containing medium, and measured IL-17 and IFNγ levels in the supernatants by ELISA. IL-17 production was detected in CII-reactive CD4+ T cells from B6 mice and in DCs from T-bet–Tg mice. Interestingly, IL-17 production was significantly reduced, even when CD4+ T cells from T-bet–Tg mice were cocultured with DCs from B6 mice (Figure 5A). These observations suggest that T-bet overexpression on CD4+ T cells is responsible for the inhibition of CII-reactive IL-17 production. No difference in IFNγ production was noted among the experimental conditions (Figure 5A), suggesting that reduced IFNγ production by CII-reactive CD4+ T cells from T-bet–Tg mice (Figure 2) was probably related to the reduced numbers of CD4+ T cells in draining lymph nodes. Moreover, intracellular staining revealed that RORγt expression was suppressed and T-bet expression was increased, even when CD4+ T cells from T-bet–Tg

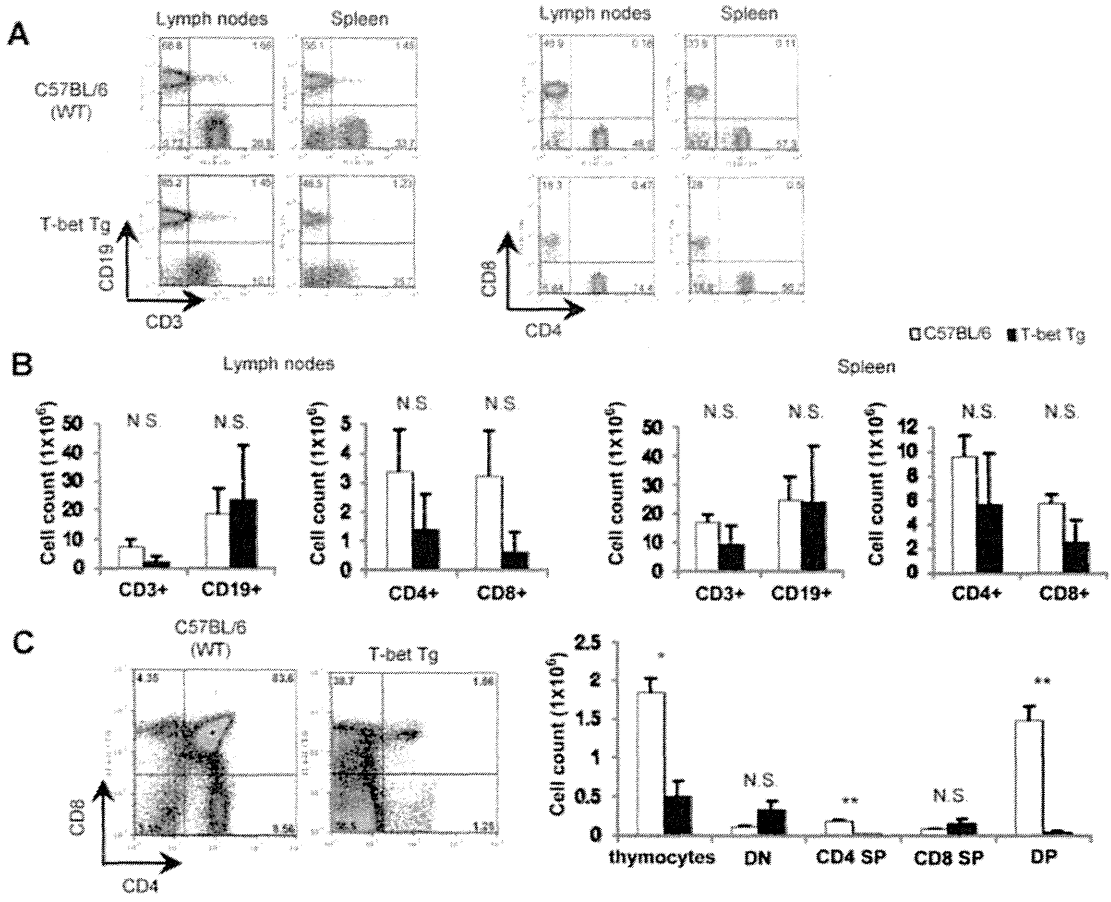

Figure 4. Decreased number of CD3+ T cells in spleen and lymph nodes and abnormal development of T precursor cells in the thymus in T-bet–transgenic (Tg) mice. **A,** Ten days after first immunization, the proportion of lymphocytes in draining lymph nodes and spleen were analyzed by fluorescence-activated cell sorting (FACS), and the absolute numbers of cells were calculated. Numbers in each compartment are the percentage of the parent population. **B,** The absolute numbers of CD3+, CD19+, CD4+, and CD8+ T cells in the lymph nodes and spleen of C57BL/6 (wild-type [WT]) and T-bet–Tg mice were determined. Values are the mean ± SD of 3 mice per group. NS = not significant. **C,** The proportion of T precursor cells in the thymus of nonimmunized mice was analyzed by FACS, and the absolute numbers of thymocytes, double-negative (DN) T cells, CD4 and CD8 single-positive (SP) T cells, and double-positive (DP) T cells were determined. Values in the bar graphs are the mean ± SD of 3 mice per group. * = $P < 0.05$; ** = $P < 0.01$ by Student's *t*-test.

mice were cocultured with DCs from B6 mice (Figure 5B). These results indicate that T-bet overexpression on CD4+ T cells suppressed CII-reactive IL-17 production by inhibition of the expression of RORγt.

Overexpression of T-bet directly suppresses Th17 cell differentiation via IFNγ-independent mechanisms. To clarify whether IFNγ production influences Th17 cell differentiation, we generated T-bet–Tg/IFNγ$^{-/-}$ mice. CD4+ T cells were isolated from the spleen of T-bet–Tg, T-bet–Tg/IFNγ$^{-/-}$, and B6 mice and were then cultured for Th17 cell differentiation. FACS analysis demonstrated that the proportion of IL-17–producing CD4+ T cells was lower in T-bet–Tg mice than in B6 mice, whereas the proportion of IFNγ-producing CD4+ T cells was higher in T-bet–Tg mice. Similarly, the proportion of IL-17–producing CD4+ T cells was also lower in T-bet–Tg/IFNγ$^{-/-}$ mice, although no IFNγ-producing CD4+ T cells were detected in

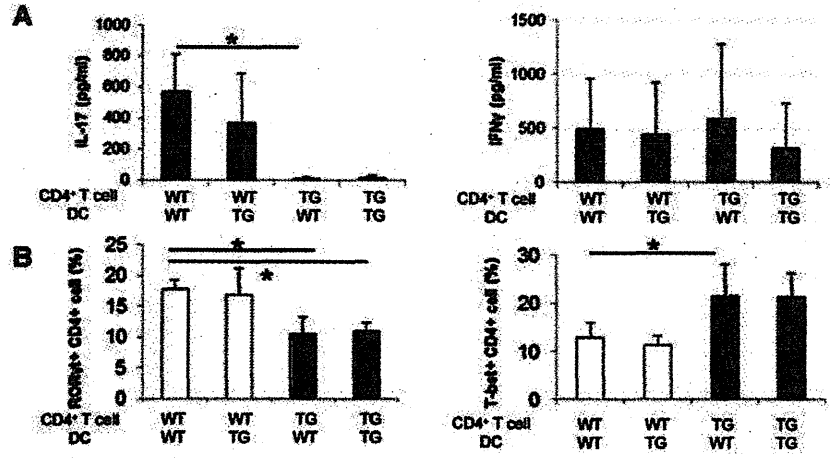

Figure 5. Impaired antigen-specific Th17 cell responses in T-bet–transgenic (Tg) mice with collagen-induced arthritis (CIA). Ten days after the first type II collagen (CII) immunization, CD4+ cells were isolated from draining lymph nodes of C57BL/6 (wild-type [WT]) mice and T-bet–Tg (TG) mice by positive selection using magnetic-activated cell sorting (MACS) with anti-CD4 monoclonal antibody (mAb). After treatment with mitomycin C, CD11c+ cells were isolated from the spleen by positive selection using a MACS system with anti-CD11c mAb. Criss-cross coculture for 72 hours was performed with 1×10^5 CD4+ cells and 2×10^4 CD11c+ cells in 100 μg/ml of denatured CII–containing medium. **A**, Levels of interleukin-17 (IL-17) and interferon-γ (IFNγ) in culture supernatants were measured by enzyme-linked immunosorbent assay. **B**, Expression of retinoic acid receptor–related orphan nuclear receptor γt (RORγt) and T-bet expression on CD4+ T cells were analyzed by intracellular staining. Representative data from flow cytometric analysis of the percentage of RORγt+ or T-bet+ cells in the CD4+ T cell subset are shown. Values are the mean ± SD of 3 mice per group. * = $P < 0.05$ by Student's *t*-test. DC = dendritic cells.

T-bet–Tg/IFNγ$^{-/-}$ mice (Figure 6). These results strongly support the view that inhibition of Th17 cell differentiation in T-bet–Tg mice cannot be due to overproduction of IFNγ, indicating that overexpression of T-bet directly suppresses Th17 cell differentiation in T-bet–Tg mice.

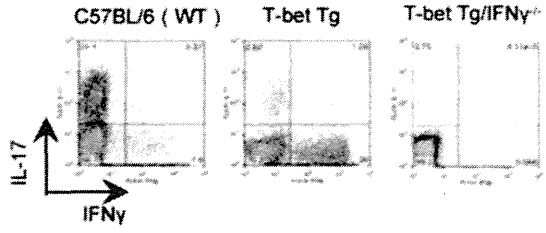

Figure 6. Suppressed expression of interleukin-17 (IL-17) by T-bet overexpression independently of interferon-γ (IFNγ) in T-bet–transgenic (Tg) mice. CD4+ T cells were isolated from the spleen of C57BL/6 (wild-type [WT]), T-bet–Tg, and T-bet–Tg/IFNγ$^{-/-}$ mice by magnetic-activated cell sorting and then cultured for 96 hours with soluble anti-CD3 monoclonal antibody (mAb), soluble anti-CD28 mAb, IL-6, and transforming growth factor β. IFNγ and IL-17 production by CD4+ cells was analyzed by intracellular cytokine staining. Numbers in each compartment are the percentage of cells secreting cytokines.

DISCUSSION

Recent studies showed that IL-17 plays a crucial role in the development of CIA (3) and other types of experimental arthritis (2). In contrast, it has been reported that IFNγ can suppress IL-17 production in vitro (16) and has antiinflammatory effects on the development of experimental arthritis (4,5). T-bet is a transcription factor known to induce the differentiation of naive CD4+ T cells to Th1 cells (8). Although the absence of T-bet can result in severe IL-17–mediated experimental autoimmune myocarditis via dysregulation of IFNγ (17), several studies have shown that T-bet is essential for the development of several models of autoimmunity, such as experimental autoimmune encephalitis (18,19), colitis (20), and diabetes mellitus (21). Nevertheless, the effect of T-bet expression on Th17 cell differentiation and function during arthritis remains unclear.

T-bet–Tg mice overexpress T-bet and mainly produce IFNγ in their T cells (14). Previous studies in T-bet–Tg mice suggested that overexpression of T-bet and a predominant Th1 response affect the pathogenesis of various diseases (14,22,23). To examine whether T-bet overexpression on T cells affects the regulation of

autoimmune arthritis, we induced CIA in T-bet–Tg mice and found marked suppression of CIA in T-bet–Tg mice.

To determine the reason for the low incidence of CIA in T-bet–Tg mice, we measured CII-reactive cytokine production and expression in vitro. IL-17 production from CII-reactive CD4+ T cells and *Il17a* expression were reduced in T-bet–Tg mice as compared with B6 mice. Although a predominant Th1 cell response was reported by Ishizuka et al (14), CII-specific IFNγ production was reduced in T-bet–Tg mice, and no significant difference was observed in *Ifng* expression between B6 mice and T-bet–Tg mice. Furthermore, *Il12a* expression was significantly higher in T-bet–Tg mice than in B6 mice, suggesting that overexpression of T-bet on T cells seems to affect innate immune cells, because the main producers of IL-12 are DCs and macrophages, not CD4+ T cells.

In criss-cross coculture experiments with CD4+ T cells and splenic DCs from B6 mice and T-bet–Tg mice, CII-reactive IL-17 production was also reduced even when CD4+ T cells from T-bet–Tg mice were cocultured with DCs from B6 mice, although there was no significant difference in IL-17 production by CD4+ T cells from B6 mice cocultured with DCs from either B6 mice or T-bet–Tg mice. In contrast, no difference in IFNγ production was observed under all coculture conditions examined. Moreover, suppression of RORγt expression and high expression of T-bet on CD4+ T cells were observed even when CD4+ T cells from T-bet–Tg mice were cocultured with DCs from B6 mice. These findings indicate that T-bet overexpression on CD4+ T cells might suppress CII-reactive IL-17 production resulting from suppression of RORγt expression in an IFNγ-independent manner, and that overexpression of T-bet has no direct effect on DC function.

CII-specific IgG levels correlate well with the development of arthritis (15). We observed significant suppression of CII-specific IgG production in the T-bet–Tg mice as compared with the B6 mice. A previous study showed that IL-17 is required for anti-CII antibody production (3). Therefore, the suppression of anti-CII antibody formation might be due to lower CII-reactive IL-17 production in T-bet–Tg mice.

To evaluate the low cytokine response to CII in T-bet–Tg mice, we analyzed lymphocytes obtained after immunization from draining lymph nodes and spleen. The percentage and absolute number of T cells tended to be lower in both the draining lymph nodes and spleen of T-bet–Tg mice compared with B6 mice. Moreover, significantly lower numbers of total thymocytes and an abnormal proportion of T precursor cells were observed in T-bet–Tg mice. The latter phenomenon could be due to T-bet transgene expression on double-negative thymic cells in T-bet–Tg mice. Because previous observations showed that T-bet interferes with GATA-3 function (11) and that GATA-3 was required for the development of early thymic T cells (24), one of the reasons for abnormal T cell development in the thymus might be the dysfunction of GATA-3 by overexpression of T-bet. These results suggest that overexpression of T-bet in thymic T cells affects T cell development, is responsible for the low number of T cells in spleen and lymph nodes, and is related to the low cytokine production against CII in T-bet–Tg mice.

To assess the effect of T-bet on CD4+ T cell differentiation in T-bet–Tg mice, we performed in vitro induction of Th17 cells. Analysis of T-bet–Tg mice showed a reduction in IL-17–producing CD4+ T cells and an increase in IFNγ-producing CD4+ T cells in spite of the condition favoring Th17 differentiation, which indicates suppression of Th17 cell differentiation and predominance of Th1 cell differentiation in vitro in T-bet–Tg mice. These results did not contradict the previous findings that the phenotype of polarized Th1 cells was not affected by Th cell–polarizing conditions (25). It is possible that suppression of CII-reactive IL-17 production in T-bet–Tg mice was not associated with IFNγ. For this reason, we generated T-bet–Tg/IFNγ$^{-/-}$ mice and performed in vitro induction of Th17 cells in these mice. Surprisingly, in T-bet–Tg/IFNγ$^{-/-}$ mice, the levels of IL-17–producing CD4+ T cells were also markedly reduced under Th17 cell differentiation–favoring conditions, indicating an IFNγ-independent suppressive pathway against Th17 cell differentiation. Although previous studies showed that suppression of Th17 cell differentiation was mediated through IFNγ signal transduction (16), our findings allow us to propose a new hypothesis: Th17 cell differentiation is regulated by a pathway that is distinct from the IFNγ signaling pathway. Therefore, we suggest that T-bet expression either directly or indirectly suppresses Th17 cell differentiation via an IFNγ-independent mechanism.

Tbx21 expression was significantly higher in T-bet–Tg mice as compared with B6 mice, and FACS analysis of CII-reactive CD4+ T cells revealed a significantly higher percentage of T-bet+ cells among the CD4+ T cell subset in T-bet–Tg mice. While there was no significant difference in the percentage of RORγt+ cells among the CD4+ T cell subset in T-bet–Tg mice as compared with B6 mice, *Rorc* expression was down-regulated on CII-reactive CD4+ T cells in T-bet–Tg mice. In the case of CD4+ T cells under

conditions favoring Th17 cell differentiation, RORγt expression on CD4+ T cells from T-bet–Tg mice was lower than that on cells from B6 mice. Interestingly, most of the RORγt+ cells also expressed T-bet in T-bet–Tg mice, and the proportion of IL-17–producing RORγt+ T cells in the CD4+ cell subset was lower in T-bet–Tg mice than in B6 mice. These findings support the notion that overexpression of T-bet not only suppresses RORγt expression on CD4+ T cells, but also inhibits the production of IL-17 from RORγt+ T cells.

Previous studies showed that RORγt expression is positively regulated by several transcription factors, such as runt-related transcription factor 1 (RUNX-1), interferon regulatory factor 4, and STAT-3 (26–28). Lazarevic et al (29) recently reported that T-bet prevented RUNX-1–mediated activation of the gene encoding RORγt, followed by the suppression of Th17 cell differentiation. In addition to direct promotion of RORγt expression, RUNX-1 also acts as a coactivator, together with RORγt, and induces the expression of *Il17a* and *Il17f* (26); therefore, T-bet inhibits IL-17 production by RORγt+ cells induced by RUNX-1 (29). Although further studies will be required to identify the effect of T-bet overexpression on the function of RUNX-1, it might be associated with the suppression of Th17 cell differentiation that was observed in the T-bet–Tg mice.

In conclusion, our results demonstrated that overexpression of T-bet in T cells suppressed the development of autoimmune arthritis. The regulatory mechanism of CIA might involve dysfunction of CII-reactive Th17 cell differentiation by overexpression of T-bet via IFNγ-independent pathways. These findings should enhance our understanding of the pathogenesis of autoimmune arthritis and help in the development of new therapies for RA.

ACKNOWLEDGMENT

We thank Dr. F. G. Issa for critical reading of the manuscript.

AUTHOR CONTRIBUTIONS

All authors were involved in drafting the article or revising it critically for important intellectual content, and all authors approved the final version to be published. Dr. Sumida had full access to all of the data in the study and takes responsibility for the integrity of the data and the accuracy of the data analysis.

Study conception and design. Sugihara, Hayashi, Yoh, Takahashi, Matsumoto, Sumida.

Acquisition of data. Kondo, Yao, Tahara.

Analysis and interpretation of data. Kondo, Iizuka, Wakamatsu, Tsuboi, Matsumoto.

REFERENCES

1. Miltenburg AM, van Laar JM, de Kuiper R, Daha MR, Breedveld FC. T cells cloned from human rheumatoid synovial membrane functionally represent the Th 1 subset. Scand J Immunol 1992;35: 603–10.
2. Iwanami K, Matsumoto I, Tanaka-Watanabe Y, Inoue A, Mihara M, Ohsugi Y, et al. Crucial role of the interleukin-6/interleukin-17 cytokine axis in the induction of arthritis by glucose-6-phosphate isomerase. Arthritis Rheum 2008;58:754–63.
3. Nakae S, Nambu A, Sudo K, Iwakura Y. Suppression of immune induction of collagen-induced arthritis in IL-17-deficient mice. J Immunol 2003;171:6173–7.
4. Chu CQ, Swart D, Alcorn D, Tocker J, Elkon KB. Interferon-γ regulates susceptibility to collagen-induced arthritis through suppression of interleukin-17. Arthritis Rheum 2007;56:1145–51.
5. Geboes L, De Klerck B, Van Balen M, Kelchtermans H, Mitera T, Boon L, et al. Freund's complete adjuvant induces arthritis in mice lacking a functional interferon-γ receptor by triggering tumor necrosis factor α–driven osteoclastogenesis. Arthritis Rheum 2007;56:2595–607.
6. Chabaud M, Durand JM, Buchs N, Fossiez F, Page G, Frappart L, et al. Human interleukin-17: a T cell–derived proinflammatory cytokine produced by the rheumatoid synovium. Arthritis Rheum 1999;42:963–70.
7. Shen H, Goodall JC, Gaston JS. Frequency and phenotype of peripheral blood Th17 cells in ankylosing spondylitis and rheumatoid arthritis. Arthritis Rheum 2009;60:1647–56.
8. Szabo SJ, Kim ST, Costa GL, Zhang X, Fathman CG, Glimcher LH. A novel transcription factor, T-bet, directs Th1 lineage commitment. Cell 2000;100:655–69.
9. Afkarian M, Sedy JR, Yang J, Jacobson NG, Cereb N, Yang SY, et al. T-bet is a STAT1-induced regulator of IL-12R expression in naive $CD4^+$ T cells. Nat Immunol 2002;57:549–57.
10. Ivanov II, McKenzie BS, Zhou L, Tadokoro CE, Lepelley A, Lafaille JJ, et al. The orphan nuclear receptor RORγt directs the differentiation program of proinflammatory IL-17+ T helper cells. Cell 2006;126:1121–33.
11. Hawng ES, Szabo SJ, Schwartzberg PL, Glimcher LH. T helper cell fate specified by kinase-mediated interaction of T-bet with GATA-3. Science 2005;307:430–3.
12. Zhou L, Lopes JE, Chong MM, Ivanov II, Min R, Victora GD, et al. TGF-β-induced Foxp3 inhibits T_H17 cell differentiation by antagonizing RORγt function. Nature 2008;453:236–41.
13. Buttgereit F, Zhou H, Kalak R, Gaber T, Spies CM, Huscher D, et al. Transgenic disruption of glucocorticoid signaling in mature osteoblasts and osteocytes attenuates K/BxN mouse serum–induced arthritis in vivo. Arthritis Rheum 2009;60:1998–2007.
14. Ishizaki K, Yamada A, Yoh K, Nakano T, Shimohata H, Maeda A, et al. Th1 and type 1 cytotoxic T cells dominate responses in T-bet overexpression transgenic mice that develop contact dermatitis. J Immunol 2007;178:605–12.
15. Cho YG, Cho ML, Min SY, Kim HY. Type II collagen autoimmunity in a model of human rheumatoid arthritis. Autoimmun Rev 2007;7:65–70.
16. Tanaka K, Ichiyama K, Hashimoto M, Yoshida H, Takimoto T, Takaesu G, et al. Loss of suppressor of cytokine signaling 1 in helper T cells leads to defective Th17 differentiation by enhancing antagonistic effects of IFN-γ on STAT3 and Smads. J Immunol 2008;180:3746–56.
17. Kiwamoto T, Ishii Y, Morishima Y, Yoh K, Maeda A, Ishizaki K, et al. Transcription factor T-bet and GATA-3 regulate development of airway remodeling. Am J Respir Crit Care Med 2006;174: 142–51.
18. Shimohata H, Yamada A, Yoh K, Ishizaki K, Morito N, Yamagata K, et al. Overexpression of T-bet in T cells accelerates auto-

immune glomerulonephritis in mice with a dominant Th1 background. J Nephrol 2009;22:123–9.
19. Rangachari M, Mauermann N, Marty RR, Dirnhofer S, Kurrer MO, Komnenovic V, et al. T-bet negatively regulates autoimmune myocarditis by suppressing local production of interleukin 17. J Exp Med 2006;203:2009–19.
20. Nath N, Prasad R, Giri S, Singh AK, Singh I. T-bet is essential for the progression of experimental autoimmune encephalomyelitis. Immunology 2006;118:384–91.
21. Yang Y, Weiner J, Liu Y, Smith AJ, Huss DJ, Winger R, et al. T-bet is essential for encephalitogenicity of both Th1 and Th17 cells. J Exp Med 2009;206:1549–64.
22. Neurath MF, Weigmann B, Finotto S, Glickman J, Nieuwenhuis E, Iijima H, et al. The transcription factor T-bet regulates mucosal T cell activation in experimental colitis and Crohn's disease. J Exp Med 2002;195:1129–43.
23. Juedes AE, Rodrigo E, Togher L, Glimcher LH, von Herrath MG. T-bet controls autoaggressive CD8 lymphocyte responses in type 1 diabetes. J Exp Med 2004;199:1153–62.
24. Hosoya T, Kuroha T, Moriguchi T, Cummings D, Maillard I, Lim KC, et al. GATA-3 is required for early T lineage progenitor development. J Exp Med 2009;206:2987–3000.
25. Shi G, Wang Z, Jin H, Chen YW, Wang Q, Qian Y. Phenotype switching by inflammation-inducing polarized Th17 cells, but not by Th1 cells. J Immunol 2008;181:7205–13.
26. Zhang F, Meng G, Strober W. Interactions among the transcription factors Runx1, RORγt and Foxp3 regulate the differentiation of interleukin 17–producing T cells. Nat Immunol 2008;9:1297–306.
27. Brustle A, Heink S, Huber M, Rosenplanter C, Stadelmann C, Yu P, et al. The development of inflammatory T_H-17 cells requires interferon-regulatory factor 4. Nat Immunol 2007;8:958–66.
28. Durant L, Watford WT, Ramos HL, Laurence A, Vahedi G, Wei L, et al. Diverse targets of the transcription factor STAT3 contribute to T cell pathogenicity and homeostasis. Immunity 2010;32:605–15.
29. Lazarevic V, Chen X, Shim JH, Hwang ES, Jang E, Bolm AN, et al. T-bet represses T_H17 differentiation by preventing Runx1-mediated activation of the gene encoding RORγt. Nat Immunol 2011;12:96–104.

OPEN ACCESS Freely available online

PLOS | ONE

Activation of Invariant NKT Cells with Glycolipid Ligand α-Galactosylceramide Ameliorates Glucose-6-Phosphate Isomerase Peptide-Induced Arthritis

Masanobu Horikoshi[1], Daisuke Goto[1], Seiji Segawa[1], Yohei Yoshiga[2], Keiichi Iwanami[1], Asuka Inoue[1], Yuki Tanaka[1], Isao Matsumoto[1], Takayuki Sumida[1]*

1 Department of Internal Medicine, Faculty of Medicine, University of Tsukuba, Tsukuba, Japan, **2** Department of Internal Medicine, University of New Mexico, Albuquerque, New Mexico, United States of America

Abstract

Objective: Invariant natural killer T (iNKT) cells regulate collagen-induced arthritis (CIA) when activated by their potent glycolipid ligand, alpha-galactosylceramide (α-GalCer). Glucose-6-phosphate isomerase (GPI)-induced arthritis is a closer model of human rheumatoid arthritis based on its association with CD4+ T cells and cytokines such as TNF-α and IL-6 than CIA. Dominant T cell epitope peptide of GPI (GPI325-339) can induce arthritis similar to GPI-induced arthritis. In this study, we investigated the roles of activation of iNKT cells by α-GalCer in GPI peptide-induced arthritis.

Methods: Arthritis was induced in susceptible DBA1 mice with GPI peptide and its severity was assessed clinically. The arthritic mice were treated with either the vehicle (DMSO) or α-GalCer. iNKT cells were detected in draining lymph nodes (dLNs) by flow cytometry, while serum anti-GPI antibody levels were measured by enzyme-linked immunosorbent assay. To evaluate GPI peptide-specific cytokine production from CD4+ T cells, immunized mice were euthanized and dLN CD4+ cells were re-stimulated by GPI-peptide in the presence of antigen-presenting cells.

Results: α-GalCer induced iNKT cell expansion in dLNs and significantly decreased the severity of GPI peptide-induced arthritis. In α-GalCer-treated mice, anti-GPI antibody production (total IgG, IgG1, IgG2b) and IL-17, IFN-γ, IL-2, and TNF-α produced by GPI peptide-specific T cells were significantly suppressed at day 10. Moreover, GPI-reactive T cells from mice immunized with GPI and α-GalCer did not generate any cytokines even when these cells were co-cultured with APC from mice immunized with GPI alone. *In vitro* depletion of iNKT cells did not alter the suppressive effect of α-GalCer on CD4+ T cells.

Conclusion: α-GalCer significantly suppressed GPI peptide-induced arthritis through the suppression of GPI-specific CD4+ T cells.

Citation: Horikoshi M, Goto D, Segawa S, Yoshiga Y, Iwanami K, et al. (2012) Activation of Invariant NKT Cells with Glycolipid Ligand α-Galactosylceramide Ameliorates Glucose-6-Phosphate Isomerase Peptide-Induced Arthritis. PLoS ONE 7(12): e51215. doi:10.1371/journal.pone.0051215

Editor: Oliver Frey, University Hospital Jena, Germany

Received July 24, 2012; **Accepted** October 30, 2012; **Published** December 12, 2012

Funding: This study was supported in part by Grants-in-Aid for Scientific Research from the Japanese Ministry of Health, Labour and Welfare and from the Ministry of Education, Culture, Sports, Science and Technology. The funders had no role in study design, data collection and analysis, decision to publish, or preparation of the manuscript.

Competing Interests: The authors have declared that no competing interests exist.

* E-mail: tsumida@md.tsukuba.ac.jp

Introduction

Rheumatoid arthritis (RA) is a chronic polyarthritic inflammatory disease of the synovial membranes. Although the etiology of RA is considered to be an autoimmune reactivity to certain self antigens, the exact mechanism remains obscure. Accumulating evidence suggests that CD4+ helper T cells play an important role in the pathogenesis of RA [1]. Invariant natural killer T (iNKT) cells are a unique subset of T cells that co-expresses NK markers, such as NK1.1 and a highly restricted TCR repertoire, composed of a single invariant α chain (Vα14-Jα18 in mice and Vα24-Jα18 in humans), together with a limited TCR Vβ repertoire. When iNKT cells recognize glycolipid ligands presented by the class I major histocompatibility complex (MHC)–like molecule CD1d on antigen presenting cells (APCs), they rapidly respond by producing large amounts of Th1, Th2, and Th17 cytokines [2–4]. The potent exogenous ligand of iNKT cells, α-galactosylceramide (α-GalCer), has been used for the treatment of several types of murine autoimmune models such as type 1 diabetes, experimental autoimmune encephalomyelitis (EAE), and collagen-induced arthritis (CIA) [5–9]. The effects of α-GalCer on these autoimmune diseases are considered to be mediated through the induction of antigen-specific IL-10 production [8,10], foxp3+ regulatory T (Treg) cells [11,12], and regulatory dendritic cells [13]. However, the role of α-GalCer in various autoimmune diseases, including RA, remains to be elucidated.

Glucose-6-phosphate isomerase (GPI) is an arthritogenic autoantigen identified in KxB/N mice [14]. GPI can provoke arthritis in susceptible DBA1 mice [15]. GPI-induced arthritis is considered to be a closer model of human RA than CIA with

regard to its dependency on CD4+ T cells and response to biological agents, such as anti-TNF-α and anti-IL-6 receptor antibody [16,17]. GPI-induced arthritis is characterized by early-onset of clinical signs of arthritis, which usually develop around day 8, with an early peak on day14. We and Bruns et al. demonstrated previously that the major epitope of T cells in GPI-induced arthritis is human GPI325–339, and that immunization with the 15-mer peptide can provoke GPI peptide-induced arthritis, which is similar to GPI-induced arthritis [18,19].

The present study is an extension to our previous studies on the role of α-GalCer in GPI peptide-induced arthritis. The results showed that α-GalCer activated iNKT cells and provided protection against GPI peptide-induced arthritis. The results also showed that α-GalCer suppressed GPI-specific CD4+ Th1 and Th17 cell response and anti-GPI autoantibody production by B cells. Thus, in the T cell dependent arthritis model, α-GalCer seems to suppress arthritis through antigen-specific regulation, suggesting a potentially useful therapeutic strategy against human RA through iNKT cell ligands.

Materials and Methods

Mice

Male DBA/1J mice were purchased from Charles River Japan (Tokyo, Japan). The animals were kept under specific pathogen-free conditions in our animal facility and studied at 7–10 weeks of age. The Institutional Animal Care and Use Committee of the University of Tsukuba approved all the experimental protocols (Permit number: 2010–116 and 2011–119). All the surgery was performed under isoflurane anesthesia, and all the efforts were made to minimize suffering.

Reagents

α-GalCer was purchased from Funakoshi (Tokyo, Japan). The stock solution of α-GalCer was dissolved in 100% dimethyl sulfoxide (DMSO) at 1 mg/ml and diluted in phosphate-buffered saline (PBS) just before injection. The following monoclonal antibodies (mAbs) were used for flow cytometric analysis: fluorescein isothiocyanate (FITC)-conjugated anti-CD4 (clone: RM4–5; Biolegend, San Diego, CA), alexa 488-conjugated foxp3 (clone: MF-14; Biolegend), phycoerythin-cyanine- 5 (PE/Cy5)-conjugated TCRβ (clone: H57–597; Biolegend), PE/Cy5-conjugated CD3 (clone; 145–2C11; Biolegend), allophycocyanin (APC)-conjugated CD19 (clone: 6D5; Biolegend), APC-conjugated CD25 (clone: PC61; Biolegend), and PE-conjugated CD1d-tetramer (MBL International, Woburn, MA). For the loading of CD1d-tetramer, the stock solution of α-GalCer was dissolved in pyridine at 1 mg/ml. Prior to use, α-GalCer was diluted to 0.2 mg/ml with 0.9% NaCl and 0.5% polysorbate-20. PE-conjugated CD1d tetramer was loaded overnight with α-GalCer at a ratio of 20:1 at room temperature. Recombinant human GPI was prepared as described previously. GPI peptide was synthesized with 90% purity by Invitrogen (Carlsbad, CA) as described previously [18].

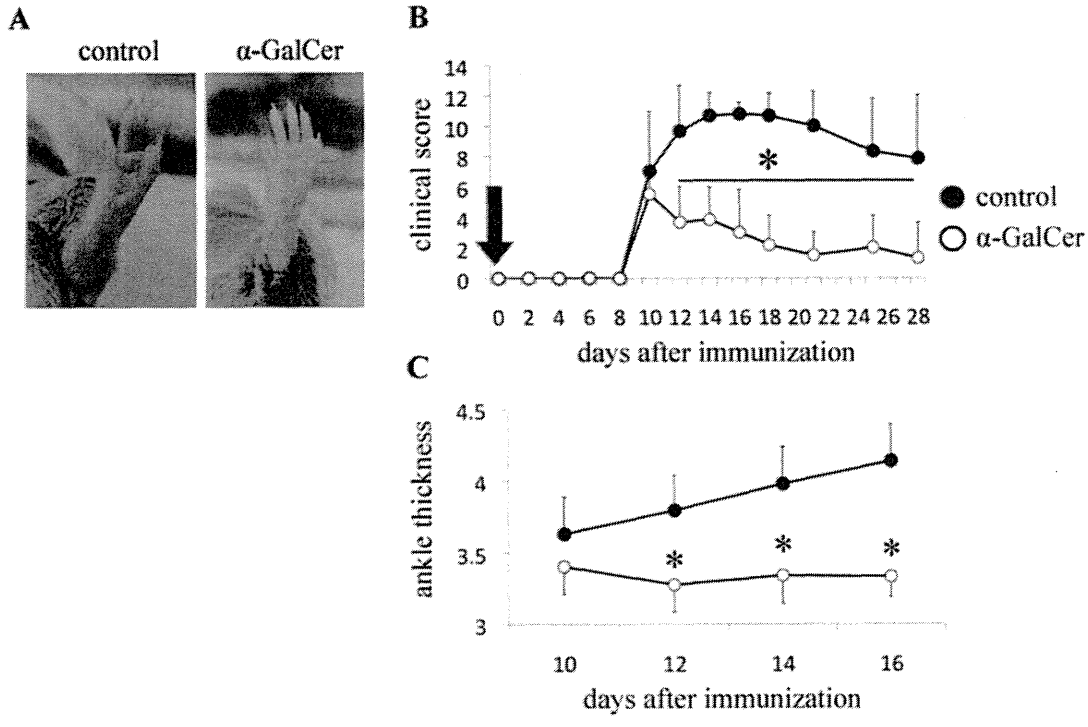

Figure 1. α-GalCer significantly suppressed the severity of GPI peptide-induced arthritis. DBA1 mice were immunized with GPI peptide and then treated with either DMSO (as a vehicle control) or α-GalCer followed by clinical assessment of arthritis. (n = 5, data shown are representative results of three experiments). (**A**) Severe swelling of ankle joints of control mice and markedly improved swelling of the ankle joints of α-GalCer-treated mice. (**B**) Clinical score, and (**C**) Ankle thickness. The latter represented the severity of arthritis. Arrow indicates α-GalCer administration. Data are mean±SD. *p<0.01, by Man-Whitney test.
doi:10.1371/journal.pone.0051215.g001

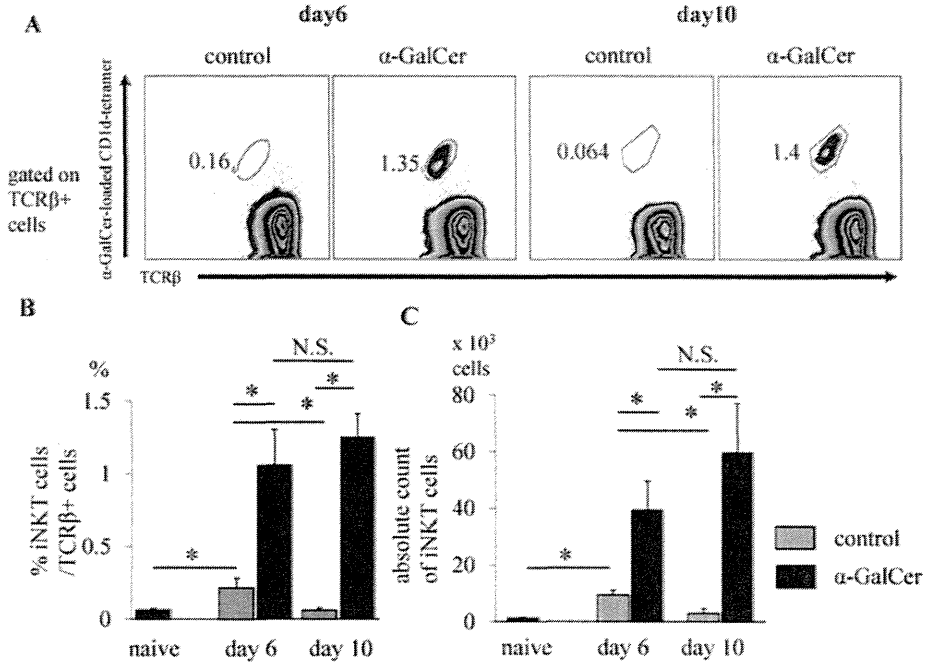

Figure 2. Expansion of iNKT cells in draining lymph nodes of α-GalCer-treated mice. Mice were immunized with GPI peptide and then treated with either DMSO or α-GalCer and euthanized on day 6 or 10. The dLNs were obtained and examined for the presence of iNKT cells by FCM (Data are mean±SD. n=4–5. Data are representative results of two experiments). **(A)** iNKT cells were detected as TCRβ and α-GalCer-loaded CD1d-tetramer double positive cells. **(B)** Proportion of iNKT cells among TCRβ+ αβT cells, and **(C)** absolute number of iNKT cells in dLNs of naive or immunized mice. *p<0.05 by Man-Whitney analysis.
doi:10.1371/journal.pone.0051215.g002

GPI Peptide-induced Arthritis and Treatment with Glycolipids

GPI peptide was dissolved in DMSO. Prior to use, GPI peptide in DMSO was dissolved in Ringer solution to appropriate volume. Mice were immunized intradermally with 10 μg of GPI peptide in complete Freund's adjuvant (CFA) (Difco, Detroit, MI). GPI peptide and CFA were emulsified at a 1:1 ratio (volume/volume). For induction of arthritis, 150 μl of the emulsion was injected intradermally into the base of the tail. On days 0 and 2 after the immunization, 200 ng of pertussis toxin (Sigma-Aldrich, St. Louis, MO) was injected into mice intraperitoneally to develop arthritis. Mice were then treated with DMSO (vehicle control of α-GalCer) or 2 μg of α-GalCer on day 0 (with GPI peptide and CFA) or day 10 (with CFA). All the α-GalCer treatments were single and intradermal injections. Arthritis was evaluated visually, and changes in each paw were scored on a scale of 0–3, as described previously [17].

Detection of Anti-GPI-antibody

Sera were obtained on day 28 and analyzed for the existence of anti-GPI antibody by enzyme-linked immunosorbent assay (ELISA). Sera were diluted 1:1000 (for IgG) or 1:100 (for IgG1, IgG2a, IgG2b, IgG3) in blocking solution (25% Block Ace (Dainippon Sumitomo Pharma, Osaka, Japan) in PBS). Then, 96-well plates were coated with 5 μg/ml of recombinant human GPI for 12 h at 4°C. After washing twice with washing buffer (0.05% Tween20 in PBS), the blocking solution was applied for 2 h at room temperature to block nonspecific binding. After 2 washes, 150 ml of diluted sera were added, and the plates were incubated for 2 h at room temperature. After three washes, horseradish peroxidase (HRP)-conjugated rabbit anti-mouse IgG (Dako, Glostrup, Denmark), IgG1 (Rockland, PA), IgG2a, IgG2b, (Zymed, San Francisco, CA), and IgG3 (Invitrogen) were added at a final concentration of 1:1000 for 1 h at room temperature. After three washes, color was developed with TMB microwell peroxidase substrate (Funakoshi). The optical density was read at 450 nm using a microplate reader.

Measurement of Serum Cytokines

Sera were obtained on days 1, 3, and 6 and analyzed for the levels of TNF-α and IL-6 by cytometric bead array (CBA) mouse inflammation kit (BD Biosciences, San Jose, CA) according to the instructions provided by the manufacturer.

Assessment of Recall Response from Antigen-specific T cells

Mice were euthanized 6 or 10 days after immunization. The draining lymph nodes (dLN) and splenocytes were isolated as described previously [20]. Single-cell suspensions were prepared in Roswell Park Memorial Institute (RPMI) 1640 medium (Sigma-Aldrich) containing 10% fetal bovine serum (FBS), penicillin–streptomycin (100 U/ml), 10 mM HEPES buffer solution (Gibco BRL, Grand Island, NY), 0.1 mM MEM nonessential amino acids (Gibco), 1 mM sodium pyruvate (Gibco), and 5.5 mM 2-mercaptoethanol (2-ME). CD4+ T cells were isolated from dLN cells by magnetic-activated cell sorting (MACS, Miltenyi Biotec, Bergisch Gladbach, Germany). The purity (more than 95%) was confirmed by flow cytometry. Splenocytes were incubated with 50 μg/ml mitomycin C (MMC) (Sigma-Aldrich) for 30 min at 37°C in a water bath.

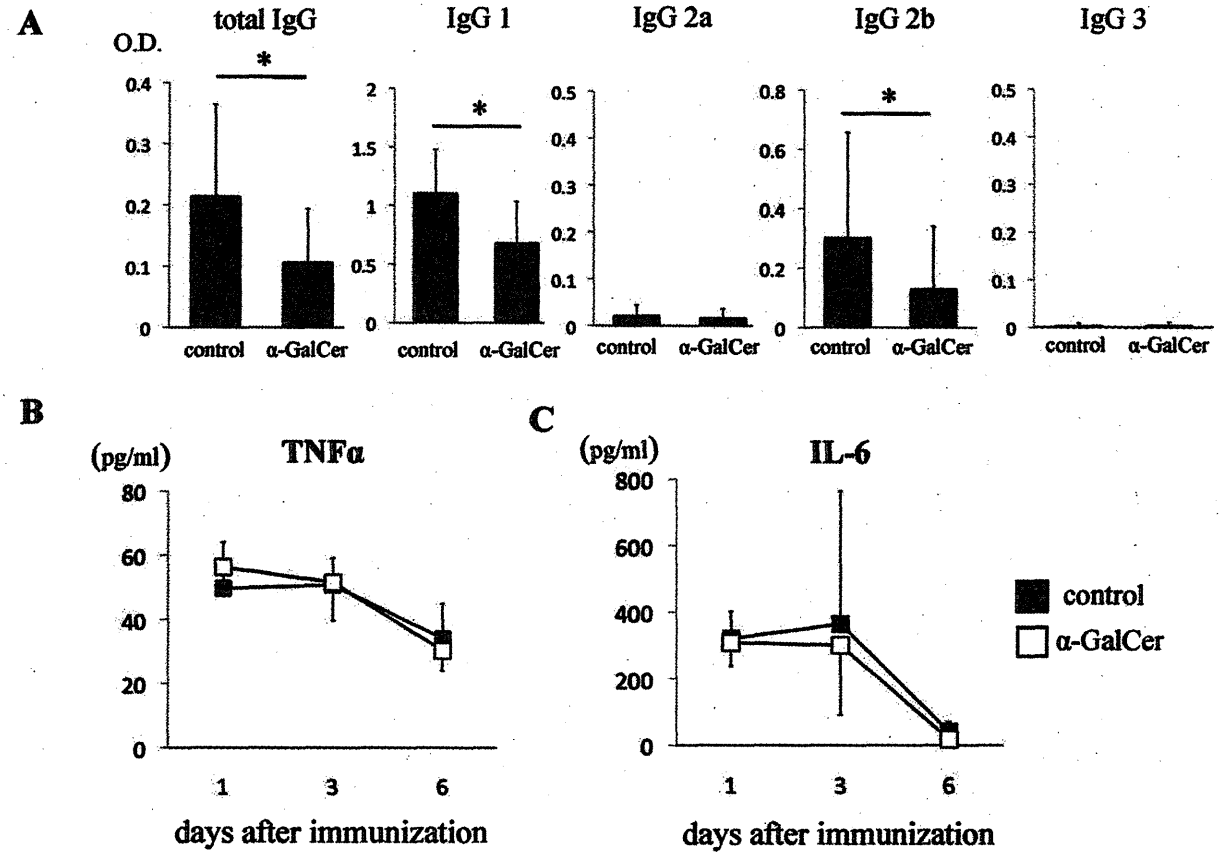

Figure 3. α-GalCer suppressed the production of autoantibodies against GPI, but not serum inflammatory cytokines. Mice were immunized with GPI peptide and treated with either DMSO or α-GalCer. Serum samples were obtained on days 1, 3, 6, and 28 after the immunization. (**A**) Levels of anti-recombinant human GPI antibody (total IgG, IgG1, IgG2a, IgG2b, IgG3) in sera obtained on day 28 were measured by ELISA (n = 11). Levels of (**B**) TNF-α and (**C**) IL-6 in the sera were measured by CBA (n = 3–5). Data are mean±SD. *p<0.05, by Man-Whitney analysis.
doi:10.1371/journal.pone.0051215.g003

Purified CD4+ T cells and MMC-treated splenocytes were co-cultured in the presence of 10 μM of GPI peptide at a ratio of 1:1 for 24 h at 37°C under 5% CO_2−95% air environment. In other experiments, MMC-treated non-T cells were used instead of splenocytes. The supernatants were assayed for IL-17, IFN-γ, IL-2, TNF-α, IL-4 and IL-10 by ELISA using Quantikine ELISA kit (R&D Systems, Minneapolis, MN).

Statistical Analysis

Values are expressed as mean ± SD. Differences between groups were examined for statistical significance using the Man-Whitney's U test. Probability values less than 0.05 were considered significant. All analyses were conducted using The Statistical Package for Social Sciences software version 19 (SPSS Inc., Chicago, IL).

Results

α-GalCer reduces the Severity of GPI Peptide-induced Arthritis

We first evaluated whether α-GalCer has a protective effect on GPI peptide-induced arthritis. Mice were intradermally immunized with GPI peptide and treated with either DMSO or α-GalCer. The severity of arthritis was evaluated by measuring the clinical score and ankle thickness. The arthritis score on day 14 was significantly lower in α-GalCer-treated mice (3.8±2.1) than in control mice (10.7±1.5, P = 0.004, **Fig. 1A and B**). Furthermore, the ankle thickness was significantly less in α-GalCer-treated mice (3.34±0.2 mm) than in control mice (3.98±0.26 mm, P = 0.008, **Fig. 1A and C**). To elucidate whether α-GalCer has protective effect against arthritis when administered after the initiation of arthritis, GPI peptide-immunized mice were intradermally administered with DMSO or α-GalCer on day 10. However, there was no significant difference between the groups (**Fig. S1**). The arthritis scores on day 14 were 9.6±1.5 in control mice, and 8.6±1.1 in α-GalCer-treated mice.

α-GalCer Induces iNKT Cell Expansion in Draining Lymph Nodes

GPI peptide-immunized mice treated with DMSO or α-GalCer were euthanized on day 6 or 10, and the dLNs were isolated and prepared for examination of iNKT cells. iNKT cells were identified as α-GalCer-loaded CD1d-tetramer and TCRβ double positive cells (**Fig. 2A**). Naive mice were also investigated for the presence of iNKT cells in the inguinal lymph nodes. The proportion and absolute number of iNKT cells in the dLNs on day 6 were significantly higher in the control peptide-treated mice

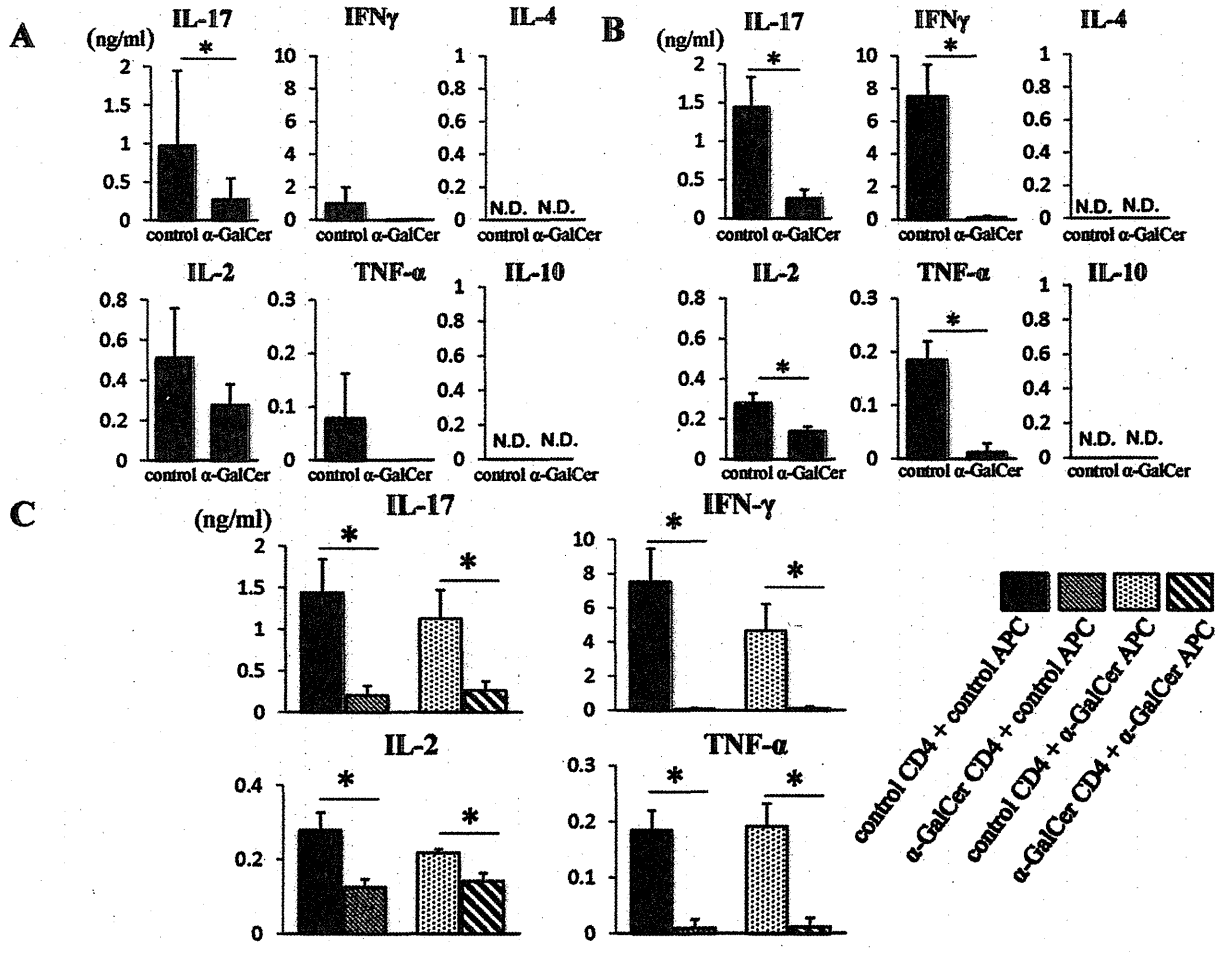

Figure 4. Suppression of antigen-specific CD4+ T cells by α-GalCer. (A)(B) Mice were immunized with GPI peptide and treated with either DMSO or α-GalCer. On day 6 (A) or day 10 (B), mice were euthanized and dLNs and spleens were harvested. CD4+ T cells were isolated from dLNs using MACS and cultured with mitomycin-treated splenocytes as antigen-presenting cells (APC). After 24-h culture, the levels of IL-17, IFN-γ, IL-2, TNF-α, IL-4 and IL-10 in the supernatant were measured by ELISA (n = 4). (C) Ten days after immunization, the mice were euthanized and dLNs and spleens were harvested. CD4+ T cells isolated from control or α-GalCer-treated mice were cultured with splenocytes (described as APC in the figure) from control or α-GalCer-treated mice. Cytokine levels in the culture supernatants were measured by ELISA (n = 4). Data are mean±SD. *p<0.05, by Man-Whitney analysis.
doi:10.1371/journal.pone.0051215.g004

(0.22±0.067%, 9.4±1.7×10^3 cells, respectively) than in naive mice (0.081±0.018%, 2.6±1.7×10^3 cells, respectively) (**Fig. 2B and C**). Surprisingly, the proportion and absolute number of iNKT cells in the dLNs were significantly higher in α-GalCer-treated mice than in control mice both on day 6 (1.1±0.24%; P = 0.021, 40±10×10^3 cells; P = 0.021, respectively) and day 10 (α-GalCer-treated mice: 1.26±0.15% and 60±17×10^3 cells, control: 0.061±0.017%, 3.0±1.7×10^3 cells, P = 0.021, respectively (**Fig. 2B and C**).

Effects of α-GalCer on GPI-specific Antibody Production

To investigate the effects of α-GalCer on GPI-specific antibody production, serum samples were obtained from control and α-GalCer-treated mice on day 28 and assayed for the levels of anti-GPI antibodies by ELISA. Since low levels of anti-GPI antibodies, especially IgG subtypes, could help identify the type of T helper cells that mediate the effect of α-GalCer, we also analyzed IgG subclasses (IgG1, 2a, 2b, 3). Administration of α-GalCer significantly reduced the production of anti-GPI antibodies of IgG, IgG1, and IgG2b compared with the control mice (IgG: 0.11±0.087 *vs* 0.21±0.15; P = 0.029, IgG1:0.68±0.35 *vs* 1.1±0.37; P = 0.014, IgG2b: 0.13±0.21 *vs* 0.30±0.35; P = 0.049, respectively) (**Fig. 3A**). These results suggest that α-GalCer suppressed antigen-specific responses independently of subsets of T helper cells, e.g., Th1 or Th2 cells.

We also analyzed the effects of α-GalCer on inflammatory cytokines on days 1, 3, and 6. Treatment with α-GalCer did not alter the serum levels of TNF-α (control: 49±14, α-GalCer: 56±5.8 pg/ml) and IL-6 (control: 321±81, α-GalCer: 309±71 pg/ml) measured on day 1 after immunization (**Fig. 3B and C**). The levels of these cytokines decreased significantly in both the DMSO- and α-GalCer-treated mice at day 6, but not at day 3 (**Fig. 3B and C**).

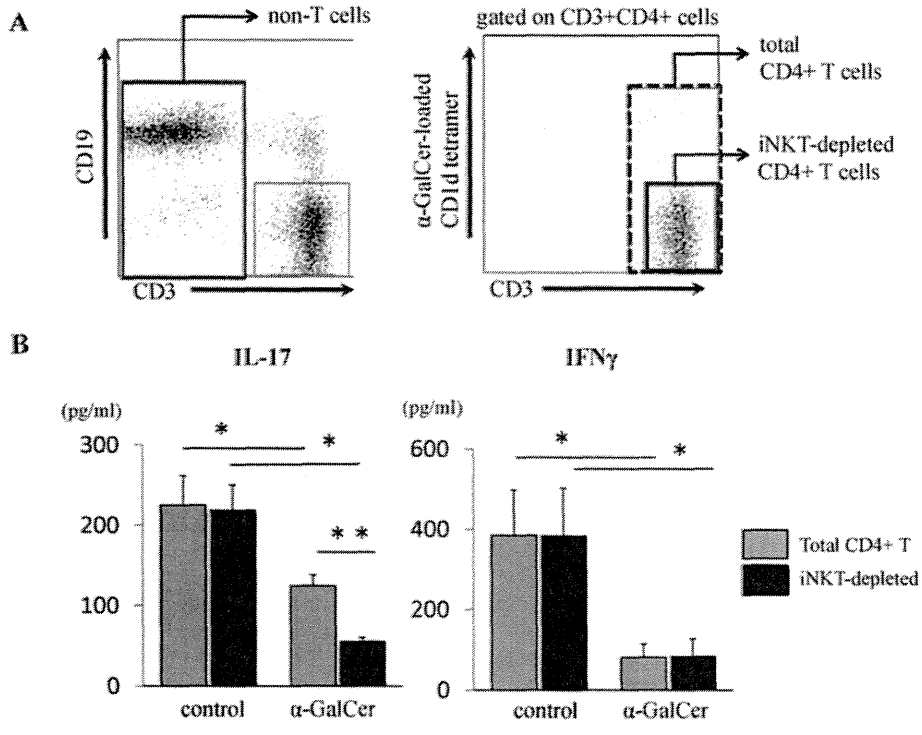

Figure 5. iNKT cells do not directly suppress antigen-specific CD4+ T cells *in vitro*. Mice were immunized with GPI peptide and treated with either DMSO or α-GalCer. Mice were euthanized on day 10 and dLNs were harvested. (**A**) Total CD4+T cells (CD3+ CD4+ cells) and NKT-depleted CD4+T cells (CD3+ CD4+ α-GalCer loaded CD1d-tetramer negative cells) were sorted by flow cytometry. These cells were cultured with sorted MMC-treated CD3-negative cells as APC in the presence of 10 μM of GPI peptide for 24 h. (**B**) Supernatants were collected and subjects to quantitative analysis of IL-17 and IFN-γ levels by ELISA. Data are mean±SD. (n=4–5). *p<0.05, **p<0.01, by Man-Whitney analysis.
doi:10.1371/journal.pone.0051215.g005

Effects of α-GalCer on GPI Peptide-specific Recall Response of CD4 T cells

The fact that GPI peptide-induced arthritis is T cell dependent, especially IL-17-producing CD4+ T cells, we also examined the effects of α-GalCer on antigen-specific CD4+ T cells. To evaluate antigen-recall response of CD4+ T cells, immunized mice were euthanized on day 6 or day 10. The isolated CD4+ T cells were co-cultured with MMC-treated whole splenocytes as APC in the presence of GPI peptide. Then, the levels of IL-17, IFN-γ, IL-2, TNF-α, IL-4, and IL-10 in the culture supernatants were measured by ELISA. On day 6, only IL-17 production was significantly suppressed in α-GalCer-treated mice (control: 1588±972 pg/ml, α-GalCer: 562±272 pg/ml; P=0.028, **Fig. 4A**). On day 10, levels of IL-17, IFN-γ, IL-2, and TNF-α were significantly lower in α-GalCer-treated mice than the control (IL-17:261±110 *vs* 1443±393 pg/ml; P=0.014, IFN-γ: 132±82 *vs* 7536±1936 pg/ml; P=0.014, IL-2:141±21.5 *vs* 279±47 pg/ml; P=0.014, TNF-α: 11.9±16.3 *vs* 185±35 pg/ml; P=0.012, respectively, **Fig. 4B**). IL-4 and IL-10 were not detected in this assay.

To determine the roles of CD4+ T cells and APCs in the above suppressive effect, CD4+ cells of the DMSO- and α-GalCer-treated mice were cultured with APCs from control or α-GalCer-treated mice in the presence of GPI peptide, then analyzed for cytokine production in response to antigen re-stimulation. Impaired recall response was noted when CD4+ T cells from α-GalCer-treated mice were cultured with APCs from control mice (IL-17:1443±393 *vs* 203±113 pg/ml; P=0.014, IFN-γ: 7536±1936 *vs* 66±60 pg/ml; P=0.028, IL-2:279±47 *vs* 125±21.5 pg/ml; P=0.025, TNF-α: 185±35 *vs* 11±15 pg/ml; P=0.022 in control CD4+control APC and α-GalCer CD4+control APC group, respectively) (**Fig. 4C**). On the other hand, no such impairment of recall response was noted when CD4+ T cells from control mice were cultured with APCs from α-GalCer-treated mice (IL-17:1124±342 *vs* 261±110 pg/ml; P=0.025, IFN-γ: 4674±1550 *vs* 132±82 pg/ml; P=0.025, IL-2:219±9.2 *vs* 141±22 pg/ml; P=0.025, TNF-α: 192±40 *vs* 12±16 pg/ml; P=0.022 in control CD4+α-GalCer APC and α-GalCer CD4+α-GalCer APC group, respectively) (**Fig. 4C**). These results suggest impairment of antigen-specific response in α-GalCer-treated mice and that CD4+ T cells are responsible for the impairment.

Recall Response of iNKT-depleted CD4+ T cells

Because dLN CD4+ T cells contain approximately 1% of iNKT cells, we questioned whether the expanding iNKT cells among dLN CD4+ T cells had direct suppressive effects on antigen-specific CD4+ T cells. To answer the question, we evaluated the recall response of iNKT-depleted CD4+ T cells. iNKT-depleted CD4+ T cells, total CD4+ T cells, and CD3- non-T cells were sorted from dLN cells of immunized mice on day 10 (**Fig. 5A**). These CD4+ T cells were cultured with non-T cells in the presence of GPI peptide. The production of IL-17 and IFN-γ was suppressed from total CD4+ cells of α-GalCer-treated mice (IL-17: control: 225±37, α-GalCer: 125±13 pg/ml; P=0.014, IFN-γ: control: 386±112, α-GalCer: 81±33 pg/ml; P=0.014) (**Fig. 5B**). The production of these cytokine was still suppressed in iNKT-

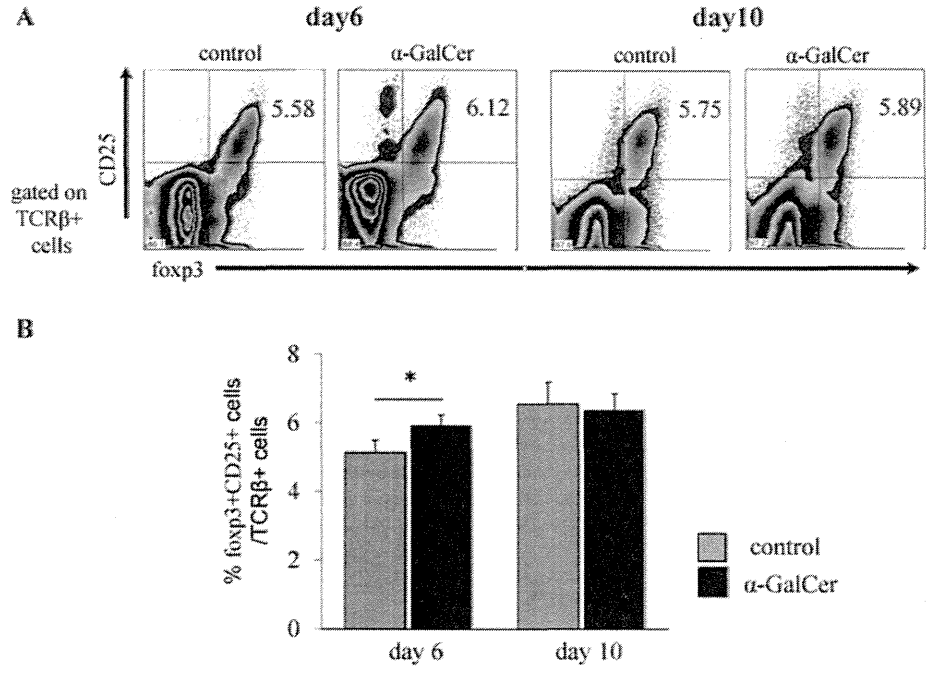

Figure 6. α-GalCer does not induce expansion of CD25+foxp3+ regulatory T (Treg) cells. Mice were immunized with GPI peptide and treated with either DMSO or α-GalCer, then euthanized on day 6 or 10 and dLN cells were harvested. (**A**) Foxp3+ T reg cells were detected as TCRβ, foxp3- and CD25-positive cells by flow cytometry. (**B**) Proportion of foxp3+ CD25+ cells among TCRβ+ αβ T cells. Data are mean±SD. *p<0.05, by Man-Whitney analysis.
doi:10.1371/journal.pone.0051215.g006

depleted CD4+ T cells from α-GalCer-treated mice (IL-17: control: 219±31, α-GalCer: 55±4.9 pg/ml; P = 0.014, IFN-γ: control: 383±120, α-GalCer: 83±44 pg/ml; P = 0.037) **(Fig. 5B)**. IL-17 production by GPI reactive T cells was significantly reduced under iNKT -depleted condition (total CD4+ T cells: 125±13, iNKT-depleted CD4+T cells: 55±4.9 pg/ml, P = 0.009) **(Fig. 5B)**. These results suggest that expanded iNKT cells did not have direct suppressive effects on antigen-specific CD4+ T cells in this assay.

Analysis of foxp3$^+$ Regulatory T cells

To determine whether induction of foxp3+ regulatory T cells mediates the suppressive effect of α-GalCer on antigen-specific CD4+ cells, we examined dLN cells of immunized mice on days 6 and 10 for the presence of foxp3+ CD25+ TCRβ+ T cells by FCM **(Fig. 6A and B)**. The proportion of foxp3+ T reg cells was significantly higher in α-GalCer-treated mice than in control mice on day 6 (control: 5.1±0.35%, α-GalCer: 5.93±0.30%, P = 0.043) but not on day10 (control: 6.6±0.62%, α-GalCer: 6.4±0.48%) **(Fig. 6B)**. However, based on the small difference, we concluded that the difference was not the reason for the potent suppressive effect of α-GalCer on pathogenic CD4+ T cells.

Discussion

GPI-induced arthritis is a newer and closer model of human RA with regard to its dependency on CD4+ T cells and reactivity to biological treatments such as blockade of IL-6 and TNF-α, which are well known to be effective in human RA. Because of its dependency on T cells, the dominant T cell epitope, which is just 15 mer peptide, can induce arthritis that resembles GPI-induced arthritis. Although accumulating evidence point to the protective role of iNKT cells against autoimmune demyelination [6,7], it is still unclear how iNKT cells work and control autoimmune arthritis, particularly through their exogenous-ligand activation. Although iNKT cells are known to promote autoimmune arthritis such as CIA, collagen-antibody induced arthritis, and K/BxN serum transfer arthritis [21], they might work differently in a ligand-specific manner. The present study was designed to explore the role of α-GalCer in GPI peptide-induced arthritis.

The results demonstrated that α-GalCer potently suppressed the severity of GPI-peptide induced arthritis. Although the severity of arthritis on day 10 was not different between the control and α-GalCer-treated mice, the former group developed more severe arthritis up to day 14 whereas α-GalCer-treated mice had a milder form of arthritis. Intradermal administration of α-GalCer with GPI peptide is delivered into dLNs by dendritic cells (DCs) residing in the skin and presented to iNKT cells by dLN DCs [22]. These facts mean that iNKT cell proliferated in the dLNs prior to the onset of arthritis. Hence, we speculated that α-GalCer-activated iNKT cells regulated GPI-specific immune response through acquisition of regulatory phenotypes or induction of regulatory cells, such as T reg cells, as reported in previous studies [11,12]. However, α-GalCer-activated iNKT cells neither induced foxp3+ CD25+ regulatory T cells nor had direct regulatory effects on antigen-specific CD4+ T cells *in vitro*. Further studies of other T reg cells might be necessary. Although iNKT cells did not have direct suppressive effects on differentiated effector T cells, they might affect helper T cell differentiation *in vivo* in the induction phase of arthritis. **Oh et al.** reported iNKT cells suppress pathogenic Th17 cells through iNKT cell - T cell interaction without cytokines in EAE [23]. It is possible that expansion of

iNKT cells in dLNs enhances the suppression of differentiation of naive T helper cells into pathogenic effector T cells.

Our previous studies [18,24] demonstrated that immunization using GPI peptide induced IL-17-producing CD4+ T cells while blockade of IL-17 resulted in amelioration of arthritis, suggesting that IL-17-producing CD4+ T cells play a pathogenic role in GPI peptide-induced arthritis. Since mice deficient in IFN-γ receptor were more resistant to GPI-induced arthritis, IFN-γ may also play a pathogenic role in GPI-induced arthritis [25]. In the present study, peptide-specific responses were significantly suppressed in α-GalCer-treated mice on day 10. These results suggest that the milder form of arthritis in α-GalCer-treated mice could have been mediated, at least in part, through the suppression of IL-17- and IFN-γ-producing T cells. **Kaieda et al.** showed that SGL-S23, an analog of α-GalCer, had suppressive effect on K/BxN serum transfer arthritis through IFN-γ [26]. We previously showed that α-carba-GalCer, an analog of α-GalCer, suppressed the severity of CIA through the induction of Th1-biased differentiation of CD4+ T cells [20]. In contrast to these studies, α-GalCer suppressed both Th1 and Th17 CD4+ T cells in GPI peptide-induced arthritis. **Coppieters et al.** reported the proliferation of IL-10-producing T cells in α-GalCer-treated mice during the course of CIA [9], and **Miellot et al.** showed that α-GalCer ameliorated CIA through the induction of IL-10-producing antigen-specific CD4+ T cells and that the protective effect was canceled by blockade of IL-10 using anti-IL-10 antibody [8]. **Chiba et al.** reported the Th2-polarizing glycolipid ligand of iNKT cells, OCH, had a potent therapeutic effect against CIA [27]. However, in our study, the protective effect of α-GalCer against arthritis was not due to the induction of antigen-specific IL-10 producing cells. Administration of α-GalCer reduced anti-GPI antibody levels independent of T helper cell subclasses. These results suggest that α-GalCer suppressed the whole antigen-specific CD4+ T cells independent of their subsets (e.g., as Th1, Th2, and Th17). In contrast to the clear effect of prophylactic administration, therapeutic α-GalCer administration on day 10 had no effect on the severity of arthritis. **Kim et al.** reported activation of iNKT cells by α-GalCer had no effect on K/BxN serum transfer arthritis in which T and B cells are not required [28,29]. These facts also suggest that the suppressive effect of α-GalCer is mediated by regulation of antigen-specific T cell development.

In conclusion, the present study demonstrated that α-GalCer significantly suppressed GPI peptide-induced arthritis through the suppression of antigen-specific CD4+ T cells. Further studies are needed to determine the mechanism through which α-GalCer-activated iNKT cells suppress the induction of antigen-specific CD4+ T cells. Such studies could advance the development of antigen-specific vaccination therapy against human RA.

Supporting Information

Figure S1 Therapeutic administration of α-GalCer had no effect on the severity of GPI peptide-induced arthritis. DBA1 mice were immunized with GPI peptide and then treated with either DMSO (as a vehicle control) or α-GalCer on day 10 followed by clinical assessment of arthritis. (n = 5). Clinical score is shown in the figure. Arrow indicates α-GalCer administration.
(TIFF)

Acknowledgments

The authors thank Dr. F. G. Issa for the critical reading of the manuscript.

Author Contributions

Conceived and designed the experiments: MH DG SS YY KI AI YT IM TS. Performed the experiments: MH. Analyzed the data: MH DG SS IM TS. Contributed reagents/materials/analysis tools: MH SS KI AI YT. Wrote the paper: MH TS.

References

1. Struyk L, Hawes GE, Chatila MK, Breedveld FC, Kurnick JT, et al. (1995) T cell receptors in rheumatoid arthritis. Arthritis Rheum 38: 577–589.
2. Bendelac A, Rivera MN, Park SH, Roark JH (1997) Mouse CD1-specific NK1 T cells: development, specificity, and function. Annu Rev Immunol 15: 535–562.
3. Godfrey DI, Hammond KJ, Poulton LD, Smyth MJ, Baxter AG (2000) NKT cells: facts, functions and fallacies. Immunol Today 21: 573–583.
4. Rachitskaya AV, Hansen AM, Horai R, Li Z, Villasmil R, et al. (2008) Cutting edge: NKT cells constitutively express IL-23 receptor and RORgammat and rapidly produce IL-17 upon receptor ligation in an IL-6-independent fashion. J Immunol 180: 5167–5171.
5. Hong S, Wilson MT, Serizawa I, Wu L, Singh N, et al. (2001) The natural killer T-cell ligand alpha-galactosylceramide prevents autoimmune diabetes in non-obese diabetic mice. Nat Med 7: 1052–1056.
6. Jahng AW, Maricic I, Pedersen B, Burdin N, Naidenko O, et al. (2001) Activation of natural killer T cells potentiates or prevents experimental autoimmune encephalomyelitis. J Exp Med 194: 1789–1799.
7. Furlan R, Bergami A, Cantarella D, Brambilla E, Taniguchi M, et al. (2003) Activation of invariant NKT cells by alphaGalCer administration protects mice from MOG35–55-induced EAE: critical roles for administration route and IFN-gamma. Eur J Immunol 33: 1830–1838.
8. Miellot A, Zhu R, Diem S, Boissier MC, Herbelin A, et al. (2005) Activation of invariant NK T cells protects against experimental rheumatoid arthritis by an IL-10-dependent pathway. Eur J Immunol 35: 3704–3713.
9. Coppieters K, Van Beneden K, Jacques P, Dewint P, Vervloet A, et al. (2007) A single early activation of invariant NK T cells confers long-term protection against collagen-induced arthritis in a ligand-specific manner. J Immunol 179: 2300–2309.
10. Mars LT, Araujo L, Kerschen P, Diem S, Bourgeois E, et al. (2009) Invariant NKT cells inhibit development of the Th17 lineage. Proc Natl Acad Sci U S A 106: 6238–6243.
11. Monteiro M, Almeida CF, Caridade M, Ribot JC, Duarte J, et al. (2010) Identification of regulatory Foxp3+ invariant NKT cells induced by TGF-beta. J Immunol 185: 2157–2163.
12. Hua J, Liang S, Ma X, Webb TJ, Potter JP, et al. (2011) The interaction between regulatory T cells and NKT cells in the liver: a CD1d bridge links innate and adaptive immunity. PLoS One 6: e27038.
13. Diana J, Brezar V, Beaudoin L, Dalod M, Mellor A, et al. (2011) Viral infection prevents diabetes by inducing regulatory T cells through NKT cell-plasmacytoid dendritic cell interplay. J Exp Med 208: 729–745.
14. Matsumoto I, Staub A, Benoist C, Mathis D (1999) Arthritis provoked by linked T and B cell recognition of a glycolytic enzyme. Science 286: 1732–1735.
15. Schubert D, Maier B, Morawietz L, Krenn V, Kamradt T (2004) Immunization with glucose-6-phosphate isomerase induces T cell-dependent peripheral polyarthritis in genetically unaltered mice. J Immunol 172: 4503–4509.
16. Matsumoto I, Zhang H, Yasukochi T, Iwanami K, Tanaka Y, et al. (2008) Therapeutic effects of antibodies to tumor necrosis factor-alpha, interleukin-6 and cytotoxic T-lymphocyte antigen 4 immunoglobulin in mice with glucose-6-phosphate isomerase induced arthritis. Arthritis Res Ther 10: R66.
17. Iwanami K, Matsumoto I, Tanaka-Watanabe Y, Inoue A, Mihara M, et al. (2008) Crucial role of the interleukin-6/interleukin-17 cytokine axis in the induction of arthritis by glucose-6-phosphate isomerase. Arthritis Rheum 58: 754–763.
18. Iwanami K, Matsumoto I, Tanaka Y, Inoue A, Goto D, et al. (2008) Arthritogenic T cell epitope in glucose-6-phosphate isomerase-induced arthritis. Arthritis Res Ther 10: R130.
19. Bruns L, Frey O, Morawietz L, Landgraf C, Volkmer R, et al. (2009) Immunization with an immunodominant self-peptide derived from glucose-6-phosphate isomerase induces arthritis in DBA/1 mice. Arthritis Res Ther 11: R117.
20. Yoshiga Y, Goto D, Segawa S, Horikoshi M, Hayashi T, et al. (2011) Activation of natural killer T cells by alpha-carba-GalCer (RCAI-56), a novel synthetic glycolipid ligand, suppresses murine collagen-induced arthritis. Clin Exp Immunol 164: 236–247.
21. Chiba A, Kaieda S, Oki S, Yamamura T, Miyake S (2005) The involvement of V(alpha)14 natural killer T cells in the pathogenesis of arthritis in murine models. Arthritis Rheum 52: 1941–1948.

22. Tripp CH, Sparber F, Hermans IF, Romani N, Stoitzner P (2009) Glycolipids injected into the skin are presented to NKT cells in the draining lymph node independently of migratory skin dendritic cells. J Immunol 182: 7644–7654.
23. Oh SJ, Chung DH (2011) Invariant NKT cells producing IL-4 or IL-10, but not IFN-gamma, inhibit the Th1 response in experimental autoimmune encephalomyelitis, whereas none of these cells inhibits the Th17 response. J Immunol 186: 6815–6821.
24. Iwanami K, Matsumoto I, Yoshiga Y, Inoue A, Kondo Y, et al. (2009) Altered peptide ligands inhibit arthritis induced by glucose-6-phosphate isomerase peptide. Arthritis Res Ther 11: R167.
25. Frey O, Mitera T, Kelchtermans H, Schurgers E, Kamradt T, et al. (2011) Ameliorated course of glucose-6-phosphate isomerase (G6PI)-induced arthritis in IFN-gamma receptor knockout mice exposes an arthritis-promoting role of IFN-gamma. J Autoimmun 36: 161–169.
26. Kaieda S, Tomi C, Oki S, Yamamura T, Miyake S (2007) Activation of invariant natural killer T cells by synthetic glycolipid ligands suppresses autoantibody-induced arthritis. Arthritis Rheum 56: 1836–1845.
27. Chiba A, Oki S, Miyamoto K, Hashimoto H, Yamamura T, et al. (2004) Suppression of collagen-induced arthritis by natural killer T cell activation with OCH, a sphingosine-truncated analog of alpha-galactosylceramide. Arthritis Rheum 50: 305–313.
28. Kim HY, Kim HJ, Min HS, Kim S, Park WS, et al. (2005) NKT cells promote antibody-induced joint inflammation by suppressing transforming growth factor beta1 production. J Exp Med 201: 41–47.
29. Kim HY, Kim S, Chung DH (2006) FcgammaRIII engagement provides activating signals to NKT cells in antibody-induced joint inflammation. J Clin Invest 116: 2484–2492.

OPEN ACCESS Freely available online

PLoS one

Genetic Polymorphisms of the Human PNPLA3 Gene Are Strongly Associated with Severity of Non-Alcoholic Fatty Liver Disease in Japanese

Takahisa Kawaguchi[1,2], Yoshio Sumida[3], Atsushi Umemura[4], Keitaro Matsuo[5], Meiko Takahashi[1], Toshinari Takamura[6], Kohichiroh Yasui[7], Toshiji Saibara[8], Etsuko Hashimoto[9], Miwa Kawanaka[10], Sumio Watanabe[11], Sumio Kawata[12], Yasuharu Imai[13], Miki Kokubo[1], Toshihide Shima[4], Hyohun Park[4], Hideo Tanaka[5], Kazuo Tajima[5], Ryo Yamada[1], Fumihiko Matsuda[1,2]*, Takeshi Okanoue[4] for the Japan Study Group of Nonalcoholic Fatty Liver Disease (JSG-NAFLD)

1 Center for Genomic Medicine, Kyoto University Graduate School of Medicine, Kyoto, Japan, **2** Institut National de la Sante et de la Recherche Medicale (INSERM) Unite U852, Kyoto University Graduate School of Medicine, Kyoto, Japan, **3** Center for Digestive and Liver Diseases, Nara City Hospital, Nara, Japan, **4** Center of Gastroenterology and Hepatology, Saiseikai Suita Hospital, Suita, Japan, **5** Division of Epidemiology and Prevention, Aichi Cancer Center, Nagoya, Japan, **6** Department of Disease Control and Homeostasis, Kanazawa University, Graduate School of Medical Science, Kanazawa, Japan, **7** Department of Molecular Gastroenterology and Hepatology, Graduate School of Medical Science, Kyoto Prefectural University of Medicine, Kyoto, Japan, **8** Department of Gastroenterology and Hepatology, Kochi Medical School, Kochi, Japan, **9** Department of Internal Medicine and Gastroenterology, Tokyo Women's Medical University, Tokyo, Japan, **10** Center of Liver Diseases, Kawasaki Hospital, Kawasaki Medical School, Okayama, Japan, **11** Department of Gastroenterology, Juntendo University School of Medicine, Tokyo, Japan, **12** Department of Gastroenterology, Yamagata University School of Medicine, Yamagata, Japan, **13** Department of Internal Medicine, Ikeda Municipal Hospital, Ikeda, Japan

Abstract

Background: Nonalcoholic fatty liver disease (NAFLD) includes a broad range of liver pathologies from simple steatosis to cirrhosis and fibrosis, in which a subtype accompanying hepatocyte degeneration and fibrosis is classified as nonalcoholic steatohepatitis (NASH). NASH accounts for approximately 10–30% of NAFLD and causes a higher frequency of liver-related death, and its progression of NASH has been considered to be complex involving multiple genetic factors interacting with the environment and lifestyle.

Principal Findings: To identify genetic factors related to NAFLD in the Japanese, we performed a genome-wide association study recruiting 529 histologically diagnosed NAFLD patients and 932 population controls. A significant association was observed for a cluster of SNPs in *PNPLA3* on chromosome 22q13 with the strongest *p*-value of 1.4×10^{-10} (OR = 1.66, 95%CI: 1.43–1.94) for rs738409. Rs738409 also showed the strongest association ($p=3.6\times10^{-6}$) with the histological classifications proposed by Matteoni and colleagues based on the degree of inflammation, ballooning degeneration, fibrosis and Mallory-Denk body. In addition, there were marked differences in rs738409 genotype distributions between type4 subgroup corresponding to NASH and the other three subgroups ($p=4.8\times10^{-6}$, OR = 1.96, 95%CI: 1.47–2.62). Moreover, a subgroup analysis of NAFLD patients against controls showed a significant association of rs738409 with type4 ($p=1.7\times10^{-16}$, OR = 2.18, 95%CI: 1.81–2.63) whereas no association was obtained for type1 to type3 ($p=0.41$). Rs738409 also showed strong associations with three clinical traits related to the prognosis of NAFLD, namely, levels of hyaluronic acid ($p=4.6\times10^{-4}$), HbA1c ($p=0.0011$) and iron deposition in the liver ($p=5.6\times10^{-4}$).

Conclusions: With these results we clearly demonstrated that Matteoni type4 NAFLD is both a genetically and clinically different subset from the other spectrums of the disease and that the *PNPLA3* gene is strongly associated with the progression of NASH in Japanese population.

Citation: Kawaguchi T, Sumida Y, Umemura A, Matsuo K, Takahashi M, et al. (2012) Genetic Polymorphisms of the Human PNPLA3 Gene Are Strongly Associated with Severity of Non-Alcoholic Fatty Liver Disease in Japanese. PLoS ONE 7(6): e38322. doi:10.1371/journal.pone.0038322

Editor: Takeshi Okanoue, Wageningen University, The Netherlands

Received March 8, 2012; **Accepted** May 3, 2012; **Published** June 14, 2012

Funding: This work was supported by the grant from Ministry of Labor and Welfare Japan [T.O., H20-Hepatitis-general-008], Core Research of Evolutional Science & Technology (CREST). The funders had no role in study design, data collection and analysis, decision to publish, or preparation of the manuscript.

Competing Interests: The authors have declared that no competing interests exist.

* E-mail: fumi@genome.med.kyoto-u.ac.jp

Introduction

Nonalcoholic fatty liver disease (NAFLD) includes a broad range of pathologies from fatty liver (simple steatosis), steatonecrosis, and steatohepatitis to cirrhosis [1–3]. NAFLD often accompanies other lifestyle-related pathologies of metabolic syndrome such as diabetes mellitus, hypertension and dyslipidemia, and the number of NAFLD patients is increasing worldwide along with the escalation in the incidence of metabolic syndrome [4]. Prevalence of NAFLD is considered as approximately 8% in Japanese and 6–35% in Europeans [4,5]. The majority of NAFLD

shows simple steatosis with a good prognosis, but approximately 10–30% of NAFLD histologically diagnosed as nonalcoholic steatohepatitis (NASH) shows hepatocyte degeneration (ballooning hepatocyte), necrosis, inflammation and fibrosis, with a higher frequency of liver-related death both in Japanese and European populations [6,7]. Insulin resistance and oxidative stress are considered to be key players in the progression of NASH [8,9]. However, the progression of NASH has been considered to be complex involving multiple genetic factors interacting with the environment and lifestyle, because only a portion of NAFLD patients develops NASH.

The first Genome-wide association (GWA) study searching for such genetic factors identified the *PNPLA3* gene as a major genetic determinant for the predisposition to NAFLD in Hispanic, African American and European American populations according to liver fat contents [10], which was subsequently confirmed in Europeans and Asians according to liver biopsy. Association of *PNPLA3* with not only fatty liver and TG content, but also inflammation and fibrosis were shown in the subsequent studies, so *PNPLA3* may be widely associated with the development of NAFLD [11–13]. More recently, another GWA study reported the association of four additional genes with NAFLD in Europeans [14]. Also, a candidate gene-based approach revealed the association between NAFLD and the apolipoprotein C3 gene in Indians [15]. However, the precise role of such genes in the development of NASH still remains to be elucidated. In addition, no GWA study has been reported for Asian populations to date although the genetic components and their relative contribution may be different between ethnicities.

The Japan NASH Study Group was founded in 2008 aiming at the identification of genetic determinants predisposing to NASH in the Japanese population. Here we report the first GWA study of NAFLD in the Japanese using DNA samples of patients with liver histology-based diagnoses recruited through this multi-institutional research network.

Results

Genome-wide Association Analysis of NAFLD in Japanese

We conducted a GWA study using DNA samples of 543 patients with NAFLD and 942 controls. After quality controls of genotyping results (see materials and methods for details), a total of 529 patients consisting of four NAFLD subgroups according to Matteoni's classification [2] (type1; 100, type2; 73, type3; 29, type4; 327) and 932 controls were subjected to statistical analyses (Table 1). This index pathologically classifies NAFLD according to the degree of inflammation, hepatocyte degeneration, and the existence of fibrosis and Mallory-Denk body in the liver. Genome scan results of 932 DNA samples collected for other genetic studies were used as general Japanese population controls [16]. After standard quality control procedure as described in materials and methods, genotype distributions of 484,751 autosomal SNP markers were compared between the NAFLD cases and control subjects by exact trend test. A slight inflation of p-values was observed by genomic control method ($\lambda = 1.04$) (Figure S1).

We identified six SNP markers located at chromosome 22q13 showing genome-wide significance ($p<1.04\times10^{-7}$) (Figure 1). Among them, four SNPs, namely, rs2896019, rs926633, rs2076211 and rs1010023, located in the *PNPLA3* gene and in strong linkage disequilibrium (LD) ($r^2>0.93$), returned p-values smaller than 1×10^{-9} ($p = 1.5\times10^{-10}$, 7.5×10^{-10}, 1.4×10^{-9} and 1.5×10^{-9}, respectively) (Table 2). Rs738407 and rs3810662 also located in *PNPLA3* showed significant but weaker associations ($p = 1.0\times10^{-7}$ and 1.0×10^{-7}, respectively) than the above four SNP markers. Rs738491, rs2073082, rs3761472, rs2235776, rs2143571 and rs6006473 were in the neighboring *SAMM50* gene which is outside of the linkage disequilibrium (LD) block where the top SNP markers were distributed (Figure 2). These markers were in moderate LD with each other ($r^2>0.42$) and showed p-values between 3.9×10^{-6} and 6.4×10^{-7} but did not reach genome-wide significance (Table S1). Rs738409, the SNP which showed the strongest association with NAFLD in the first GWA study [10], was not included in the SNP array used in our study. This SNP was therefore genotyped using Taqman technology in the same case and control samples that were used for genome scan. Rs738409 showed the strongest association with the disease ($p = 1.4\times10^{-10}$, OR = 1.66, 95%CI: 1.43–1.94) among all the SNP markers examined in this study. The association remained after the correction for population stratification with EIGENSTRAT [17] ($p = 2.3\times10^{-11}$). Although a peak consisting of a cluster of SNPs was observed at the *HLA* locus on chromosome 6 (minimal p-value of 4.10×10^{-7} for rs9262639 located at the 3′ of *C6orf15* gene), the association disappeared when EIGENSTRAT was applied ($p>1.6\times10^{-3}$). We consider this as a result of population stratification between the cases and controls.

Impact of *PNPLA3* Polymorphisms to the Pathogenicity of NAFLD

We next examined whether or not the seven SNPs in the *PNPLA3* gene were associated with the pathogenic status of NAFLD. The genotype distributions of these SNPs were compared by Jonckheere-Terpstra test among the four subgroups of NAFLD patients categorized by Matteoni's classification (type1 to type4). There was a significant increase in the frequency of the risk allele from Matteoni type1 to type4 for all of the seven SNPs (p-values ranging from 3.6×10^{-6} to 0.0017) (Table 2). Among them, rs738409 again showed the strongest association ($p = 3.6\times10^{-6}$) as seen in the simple case/control analysis. On the other hand, there was no significant association between control and Matteoni type1 ($p = 0.76$).

In order to clarify how rs738409 influences the pathogenicity of NAFLD, we performed pairwise comparisons of genotype distributions in the four subgroups of NAFLD patients. There were marked differences in genotype distributions between type4 subgroup and the other three subgroups by multivariable logistic regression adjusted for age, sex and body mass index (BMI) ($p = 2.0\times10^{-5}$, OR = 2.18, 95%CI: 1.52–3.18 between type1 and type4; $p = 1.4\times10^{-3}$, OR = 1.81, 95%CI: 1.26–2.62 between type2 and type4; $p = 0.027$, OR = 1.85, 95%CI: 1.07–3.19 between type3 and type4) (Figure 3). On the other hand, no significant associations were obtained for type1 to type3 in any combinations. When we performed the same analysis between type4 and the pooled genotypes of type1 to type3, we again obtained a significant difference ($p = 4.8\times10^{-6}$, OR = 1.96, 95%CI: 1.47–2.62).

We further examined the specific association of rs738409 with type4 subgroup by using the case/control association results of the initial genome scan. 529 NAFLD patients were divided into 202 patients with type1 to type3 and 327 patients with type4, and genotype distributions of rs738409 in each subgroup were compared with those of 932 control subjects. Exact trend test returned an extremely strong association of rs738409 with type4 subgroup ($p = 1.7\times10^{-16}$, OR = 2.18, 95%CI: 1.81–2.63) whereas no association was obtained for type1 to type3 subgroups ($p = 0.41$).

Table 1. Clinical characteristics according to the histological classification.

Phenotype	Matteoni classification of NAFLD				Control	*p*-value
	Type 1	Type 2	Type 3	Type 4		
Number of samples	100	73	29	327	932	
Sex (Male/Female)	59/41	47/26	13/16	130/197	471/461	0.0023‡
Age (year)	49.7±15.3	51.5±15.3	49.4±14.0	57.6±14.8	48.8±16.3	<0.001
Physical measurement						
BMI	26.2±4.3	27.7±4.8	27.6±3.5	27.7±5.2	–	0.054
Amount of visceral fat (cm^2)	146.8±65.3	154.3±47.7	136.8±53.8	151.7±57.4	–	0.46
Abdominal circumscript (cm)	90.9±9.9	94.1±10.0	88.5±10.2	94.1±11.8	–	0.10
Biochemical trait						
AST (IU/L)	31.1±14.6	36.4±18.5	52.4±35.1	57.7±48.4	–	<0.001
ALT (IU/L)	48.6±30.8	62.8±47.6	81.5±46.9	74.9±48.4	–	<0.001
GGT (IU/L)	71.0±62.5	67.1±66.9	96.1±91.3	76.6±73.9	–	0.25
Albumin (g/dL)	4.5±0.4	4.4±0.3	4.5±0.3	4.3±0.4	–	<0.001
Total bilirubin (mg/dL)	0.9±0.5	0.9±0.5	0.9±0.6	0.8±0.4	–	0.063
Cholinesterase (unit)	389.1±97.0	354.3±97.2	371.1±109.9	348.9±93.2	–	<0.001
Type IV collagen 7S (ng/dL)	3.8±0.7	3.9±0.9	3.9±0.8	5.1±1.7	–	<0.001
Hyaluronic acid (ng/dL)	25.6±22.5	33.6±29.5	31.5±24.0	80.9±84.3	–	<0.001
Triglycerides (mg/dL)	151.9±73.8	154.0±92.1	166.1±86.5	161.2±85.7	–	0.23
Total cholesterol (mg/dL)	209.1±32.8	194.0±38.0	203.0±39.9	200.3±39.0	–	0.093
HbA1c (%)	6.1±1.1	5.9±1.2	6.5±1.8	6.2±1.3	–	0.13
IRI (μg/dL)	9.1±5.4	11.4±9.0	10.4±6.3	14.9±9.9	–	<0.001
FPG (mg/dL)	112.9±33.7	107.3±27.4	109.9±27.7	114.8±33.8	–	0.14
HOMA-IR	2.4±1.5	2.9±2.4	3.0±2.1	4.2±3.0	–	<0.001
hs-CRP (mg/dL)	1078.9±1407	1048.3±1185.0	865.8±658.4	1579.2±2377.9	–	0.027
Adiponectin (μg/mL)	7.4±4.4	8.5±6.6	6.6±2.6	6.9±4.3	–	0.24
Leptin (ng/mL)	9.9±7.4	9.1±6.2	11.3±9.4	12.4±7.9	–	<0.001
Ferritin (ng/mL)	145.8±101.1	176.5±134.0	271.2±307.0	208.3±180.3	–	0.027
Uric acid (mg/dL)	5.9±1.5	5.7±1.2	5.4±1.9	5.7±1.6	–	0.77
PLT ($\times 10^4/\mu L$)	23.0±5.9	22.9±4.9	21.9±6.7	20.2±6.4	–	<0.001
ANA (0/1/2/3/4)	42/17/4/0/0	31/8/4/1/2	15/6/2/0/0	147/76/31/8/12	–	0.015
Clinical history						
Diabetes (NGT/IGT/DM)	36/11/34	24/7/27	12/8/7	103/35/119	–	0.45*
Hyperlipidemia (+/−)	31/68	31/42	9/20	120/206	–	0.60‡
Hypertension (+/−)	64/35	33/40	19/10	155/172	–	0.013‡
Liver biopsy feature						
Brunt grade (1/2/3)	–	–	19/3/2	149/133/44	–	<0.001‡
Brunt stage (1/2/3/4)	–	–	–	123/74/105/24	–	–
Fat droplet (1/2/3/4)	38/32/19/11	14/29/18/7	7/3/10/4	51/99/104/52	–	<0.001
Iron deposition (0/1/2/3/4)	30/14/21/10/1	24/9/12/2/1	10/5/2/2/0	132/56/29/29/11	–	0.16

Measurements are shown as mean ± standard deviation. Categorical values are shown by the count number. *P*-values are calculated by Jonckheere-Terpstra test unless otherwise stated;

‡Chochran-Armitage trend test,

*Kruskal-Wallis test. Abbreviations used for each trait are summarized in materials and methods.

doi:10.1371/journal.pone.0038322.t001

Association of rs738409 Genotypes with Clinical Traits

The quantitative effects of rs738409 genotypes to clinical traits were examined by multivariable regression adjusted for age, sex and BMI (statistical calculation 1, Table 3). Five categorical ordinals, namely, anti-nuclear antibody (ANA), Brunt grade, Brunt stage, fat deposition and iron deposition, were also tested by an ordinal logistic regression analysis. Potential associations ($p<0.05$) were obtained for 11 traits, namely, aspartate transaminase (AST), alanine aminotransferase (ALT), type IV collagen 7S, hyaluronic acid, hemoglobin A1c (HbA1c), fasting immunoreactive insulin (IRI), fasting plasma glucose (FPG), platelet count (PLT), Brunt grade, fat deposition and iron deposition (Table 3). When the results were further adjusted for Matteoni type (statistical calculation 2), AST, hyaluronic acid, HbA1c, FPG,

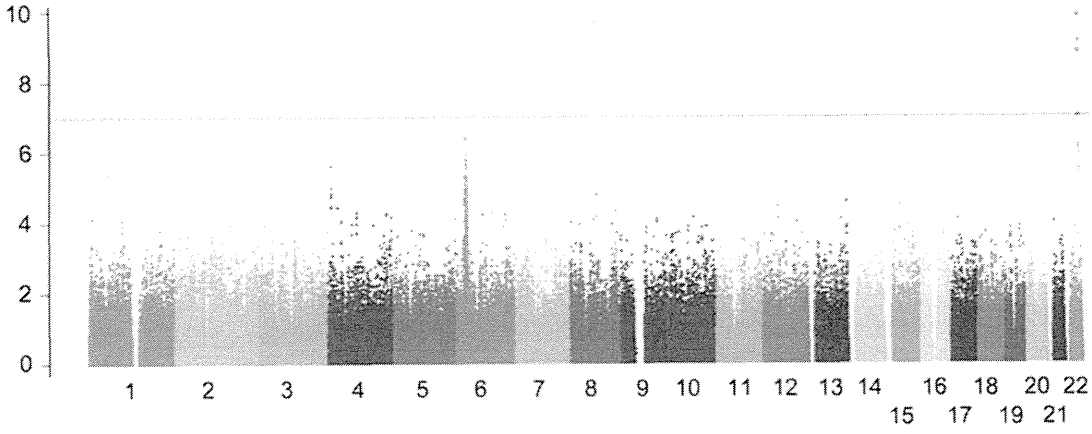

Figure 1. Manhattan plot of the GWA study. Association *p*-values are calculated by exact trend test and plotted along the chromosome in $-\log_{10}$ scale. The horizontal line indicates Bonferroni-adjusted significance threshold ($p = 1.03 \times 10^{-7}$).
doi:10.1371/journal.pone.0038322.g001

PLT, Brunt grade and iron deposition showed *p*-values smaller than 0.05. The level of serum triglyceride was not significant in the initial analysis, but became significant after being adjusted for Matteoni's type ($p = 0.013$). Among them, only three traits, namely, hyaluronic acid, HbA1c and iron deposition, remained significant ($p < 0.0021$) after Bonferroni's correction for multiple testing (Table 3).

Associations of Previously Reported SNPs with NAFLD

Previous genetic studies identified four chromosomal loci, namely, *LYPLAL1* at 1q41, *GCKR* at 2p23, *NCAN* at 19p12 and *PPP1R3B* at 8p23.1, associated with NAFLD in populations of European descent [14]. We examined whether or not the associations were reproduced in the Japanese population by extracting genotype information of SNP markers corresponding to these four loci. As shown in Table 4, the association of rs780094 in *GCKR* with NAFLD was at the border of significance ($p = 0.011$, OR = 0.82, 95%CI: 0.70–0.91) in the case/control analysis. However, the association was lost when examined between rs780094 genotypes and Matteoni types. There were no associations of rs2228603 in *NCAN* and rs12137855 in *LYPLAL1* with either NAFLD or Matteoni types. Rs4240624 in *PPP1R3B* was not in the SNP array used for this study, and this marker was not polymorphic or at a very low frequency in the Japanese (0 in 90

Table 2. List of the SNP markers in the *PNPLA3* locus at chromosome 22q showing genome wide significance.

		Genotyping Result and Allele Frequency of A2						Statistics		
			NAFLD					NAFLD vs. Control		Matteoni
dbSNPID	A1/A2	Control	Total	Type 1	Type 2	Type 3	Type 4	*p*-value†	OR (95%CI)	*p*-value‡
rs738407	T/C	124/447/361	46/200/283	12/51/37	10/28/35	4/14/11	20/107/200	1.0×10^{-7}	1.56(1.32–1.83)	3.4×10^{-5}
		(0.627)	(0.724)	(0.625)	(0.671)	(0.621)	(0.775)			
rs738409	C/G*	247/468/217	88/236/203	20/59/21	21/30/22	8/11/9	39/136/151	1.4×10^{-10}	1.66(1.43–1.94)	3.6×10^{-6}
		(0.484)	(0.609)	(0.505)	(0.507)	(0.518)	(0.672)			
rs2076211	C/T*	248/473/211	92/242/195	21/58/21	21/30/22	8/11/10	42/143/142	1.4×10^{-9}	1.61(1.38–1.87)	3.2×10^{-5}
		(0.480)	(0.597)	(0.500)	(0.507)	(0.534)	(0.653)			
rs2896019	T/G*	246/473/213	91/234/204	20/57/23	22/29/22	7/12/10	42/136/149	1.5×10^{-10}	1.66(1.42–1.93)	2.6×10^{-5}
		(0.482)	(0.607)	(0.515)	(0.500)	(0.552)	(0.664)			
rs1010023	T/C*	249/473/210	94/239/196	21/57/22	22/29/22	7/12/10	44/141/142	1.5×10^{-9}	1.61(1.38–1.87)	6.5×10^{-5}
		(0.479)	(0.596)	(0.505)	(0.500)	(0.552)	(0.650)			
rs926633	G/A*	247/474/211	93/237/199	21/56/23	22/29/22	7/12/10	43/140/144	7.5×10^{-10}	1.62(1.39–1.89)	5.8×10^{-5}
		(0.481)	(0.600)	(0.510)	(0.500)	(0.552)	(0.654)			
rs3810622	T*/C	330/445/157	263/208/58	40/48/12	28/29/16	14/12/3	181/119/27	1.0×10^{-7}	0.64(0.55–0.75)	0.0017
		(0.407)	(0.306)	(0.360)	(0.418)	(0.310)	(0.265)			

Reference (A1) and non-reference (A2) alleles refer to NCBI Reference Sequence Build 36.3 with the effective allele marked by an asterisk. Genotyping results are shown by genotype count of A1A1/A1A2/A2A2 with allele frequency of A2 in parenthesis.
†*P*-values are calculated by exact trend test with odds ratios (OR) calculated for A2 with 95% confidence interval (CI).
‡*P*-values are calculated by Jonckheere-Terpstra test in NAFLD patients for Matteoni type and additive model of genotype. SNPs are ordered by chromosomal location.
doi:10.1371/journal.pone.0038322.t002

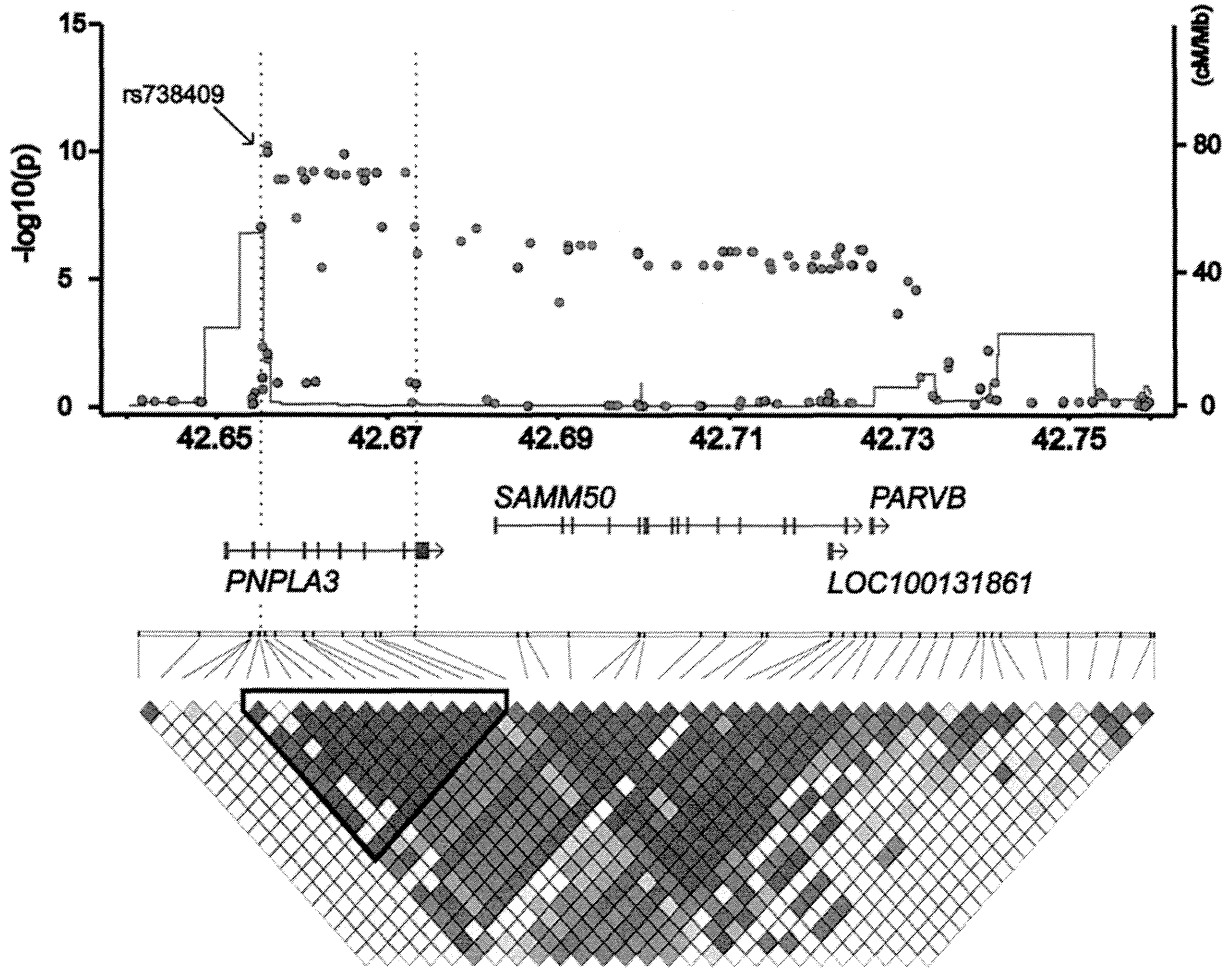

Figure 2. A schematic organization of the human *PNPLA3* locus at 22q13.31 with the genome scan results. *P*-values calculated by the exact trend test were plotted in $-\log_{10}$ scale. Red and blue dots indicate the *p*-values of genotyped and imputed SNPs, respectively. Local recombination rate obtained from HAPMAP release 22 is indicated by a red line plotted in cm/Mb scale. The structure and orientation of four genes in the region are shown below the plots with their transcriptional orientations according to NCBI Reference Sequence Build 36.3. LD blocks were generated according to pairwise LD estimates of the SNPs located within the region using the genome scan results. The LD block showing the strongest association is highlighted with the triangle, and the corresponding chromosomal region is represented by the dotted lines.
doi:10.1371/journal.pone.0038322.g002

chromosomes in the Japanese result of the International HapMap Project).

Discussion

NASH is a type of hepatic steatosis in NAFLD with poor prognosis accompanying liver fibrosis, and subsequent liver cirrhosis and hepatocellular carcinoma [18]. Despite the extensive biochemical and histological investigation of NAFLD, whether or not NASH forms a distinct disease entity in NAFLD still remains unclear. The principle aim of this study was to identify the genetic factors related to the pathogenic status of NAFLD by collecting DNA samples of Japanese NAFLD patients with critically diagnosed disease status by liver biopsy. To our knowledge, this is the first GWA study of NAFLD using patients with known histology-based Matteoni type. In the initial association study using pooled genotyping results of all the cases, we found a significant association of the *PNPLA3* gene at chromosome 22q13.31 with NAFLD in the Japanese. Rs738409 which showed the strongest association with NAFLD in the GWA study of Caucasians was also genotyped and its strongest association with NAFLD was confirmed. These results were in agreement with the former GWA analyses in populations of European descent and in Hispanics, giving strong evidence of the involvement of *PNPLA3* in NAFLD beyond ethnicities. Rs738409 is located in exon3 of the *PNPLA3* gene which is expressed in the liver and adipose tissue. This SNP introduces an amino acid substitution from isoleucine to methionine (I148M), and biological studies demonstrated that its risk allele (G) abolishes the triglyceride hydrolysis activity of *PNPLA3* [19]. These observations strongly suggest rs738409 to be a causative genetic variation for NAFLD. However, future genomic analyses by fine mapping or extensive sequencing may identify additional genetic determinants within the *PNPLA3* locus.

In the current study we did not find other genetic loci showing genome-wide significance ($p<1.0\times10^{-7}$). However, two additional chromosomal loci with *p*-values being smaller than 1×10^{-5} were